The Framework Programme for Research & Innovation
Innovation actions (IA)

Project Title:
Autonomous self powered miniaturized intelligent sensor for environmental sensing and asset tracking in smart IoT environments

AMANDA

Grant Agreement No: 825464

[H2020-ICT-2018-2020] Autonomous self powered miniaturized intelligent sensor for environmental sensing and asset tracking in smart IoT environments

Deliverable

D1.1 SoA and Gap analysis/recommendations on ESS features report

Deliverable No.		D1.1		
Workpackage No.	WP1	Workpackage Title and task type	**System Specifications, Requirements and Use Cases**	
Task No.	T1.1	Task Title	**Task 1.1: SoA Analysis, feasibility study & benchmarking of best practices**	
Lead beneficiary		**CERTH**		
Dissemination level		**PU**		
Nature of Deliverable		**R**		
Delivery date		**30 April 2019**		
Status		**Final**		
File Name:		**AMANDA D1.1_SoA_and_Gap_analysis_recommendations_on_ESS_features_report-v1.1**		
Project start date, duration		**02 January 2019, 36 Months**		

Authors List

Leading Author (Editor)			
Surname	*Initials*	*Beneficiary Name*	*Contact email*
Kouzinopoulos	CS	CERTH	kouzinopoulos@iti.gr
Co-authors (in alphabetic order)			
#	*Surname*	*Initials*	*Beneficiary Name*	*Contact email*
1	Bellanger	MB	Lightricity	mathieu.bellanger@lightricity.co.uk
2	Bembnowicz	PB	IMEC-NL	pawel.bembnowicz@imec-nl.nl
3	Govaerts	JG	EPEAS	julien.govaerts@e-peas.com
4	Haine	TH	EPEAS	thomas.haine@e-peas.com
5	Hal	RH	IMEC-NL	Roy.vanHal@imec-nl.nl
6	Hidalgo	JH	EPEAS	juan.hidalgo@e-peas.com
7	Kanlis	AK	CERTH	alexkanlis@iti.gr
8	Meli	MM	ZHAW	marcel.meli@zhaw.ch
9	Schellenberg	MS	Microdul	martin.schellenberg@microdul.com
10	Sideridis	PS	CERTH	sideridis@iti.gr

Reviewers List

List of Reviewers (in alphabetic order)			
#	*Surname*	*Initials*	*Beneficiary Name*	*Contact email*
1	Pasero	DP	Ilika	denis.pasero@ilika.com
2	De Vos	JD	EPEAS	julien.devos@e-peas.com
3	Govaerts	JG	EPEAS	Julien.govaerts@e-peas.com
4	Haine	TH	EPEAS	Thomas.haine@e-peas.com
5	Masson	SM	EPEAS	Sebastien.masson@e-peas.com

Document history			
Version	Date	Status	Modifications made by
0.1	23/01/2019	ToC	CERTH
0.2	29/03/2019	First draft with contributions from Microdul and IMEC	CERTH, Microdul, IMEC
0.3	02/04/2019	Document improvements	CERTH
0.5	11/04/2019	Added Benchmarking and Recommendations sections	CERTH
0.7	15/04/2019	Contributions from EPEAS and ZHAW	CERTH, EPEAS, ZHAW
0.8	17/04/2019	Contribution from Lightricity	Lightricity
0.9	18/04/2019	Contribution from ILIKA	ILIKA
1.0	25/04/2019	Incorporated feedback from reviewers	CERTH, ILIKA, EPEAS
1.1	08/11/2019	Additional academic State-of-the-Art including recent developments. Minor text corrections	Lightricity, IMEC, ILIKA, Microdul, EPEAS, CERTH

List of definitions & abbreviations

Abbreviation	Definition
ADC	Analog to Digital Converter
AoA	Angle of Arrival
ASSC	Autonomous Smart Sensing Card
BLE	Bluetooth Low Energy
CDC	Capacitance-to-Digital Conversion
CIS	CMOS Image Sensor
CSP	Chip-scale package
DFN	Dual flat-pack
EDA	Electrodermal Activity
EEMBC	Embedded Microprocessor Benchmark Consortium
EKG	Electrocardiogram
EMF	Electromotive Force
ESS	Electronic Smart Systems
FISA	Flexible Integrated Sensing Array
FoM	Figure of Merit
GSM	Global System for Mobile communications
IoT	Internet of Things
LED	Light Emitting Diode
LPWAN	Low-Power Wide-Area Network
LTE	Long-Term Evolution
M2M	Machine to Machine
MCU	Microcontroller Unit
MEMS	Microelectromechanical System
MID	Molded Interconnect Devices
MPPT	Maximum Power Point Tracking

PCB	Printed Circuit Board
PET	Polyethylene terephthalate
PMIC	Power Management Integrated Circuit
PV	Photovoltaic
PRB	Physical Resource Blocks
QFN	Quad flat no-leads package
R2R	Roll-to-roll
SIC	Stacked-IC
SIP	System-in-Package
SoA	State-of-the-Art
SPI	Serial Peripheral Interface
UTCP	Ultra-Thin Packaging Technology
WAN	Wide-Area Network
WLP	Wafer-level-Package
WPAN	Wireless Personal Area Network

Executive Summary

This report is part of **WP1 - System Specifications, Requirements and Use Cases** of the AMANDA project. The aim of WP1 is to provide an overall framework for the project, to ensure a common reference point regarding the system requirements that arise from use analysis and to provide overall considerations and guidelines with respect to the solutions introduced. The Deliverable presents a SoA analysis, a feasibility study as well as benchmarking of best practices that were performed as part of **Task T1.1 – SoA Analysis, feasibility study & benchmarking of best practices**, the result of a thorough investigation of different scientific and commercial resources. The recent advances in the research and development of the technologies used in the AMANDA ASSC including PV Energy Harvesters, Sensors, Batteries, MCUs and wireless communication components is performed, focusing on cutting edge technologies and solutions available today on the market, both under the pilot phase as well as under the development phase. In the latest revision of this Deliverable, additional literature on technologies and devices has been included on the main sensors of the ASSC as well as the PV energy harvester and the energy storage unit.

An in-depth GAP analysis was conducted to specify in detail the technological innovation potential for the AMANDA hardware and to introduce new, innovative features. Finally, this document proposes a list of recommendations to give further directions for the AMANDA project.

Table of Contents

List of Figures

List of Tables

1   Introduction

1.1   Purpose, Context and Scope of this Deliverable

This Deliverable presents a SoA analysis for technologies related to the AMANDA ASSC. These technologies include different PV Energy Harvesters, batteries, sensors, MCUs and protocols for wireless communication. A GAP analysis is also performed to specify in detail the technological innovation potential for the AMANDA solution and to propose new and innovative features. Moreover, a list of recommendations is proposed to give further directions for the AMANDA work as part of **Task T1.1 - SoA Analysis, feasibility study & benchmarking of best practices**. T1.1 has a focus on cutting edge technologies and solutions available on the market, under pilot stage and under development.

This document is structured as follows: Section 2 describes a SoA analysis on sensors, MCUs, energy harvesting, batteries, PMICs, wireless communication, packaging, PCB design and memory elements and introduces a benchmarking and feasibility study on ASSC sensors, developed by Partners of the AMANDA project. In Section 3, guidelines for the AMANDA work are proposed. In Section 4, a GAP analysis identifies the technological innovation potential and innovative features that will be developed during the project by all partners of the AMANDA project. Section 5 proposes recommendations to give further directions for the AMANDA project. Finally, in Section 6, the conclusions of this Deliverable are drawn and further work is discussed.

1.2   Background

The AMANDA project aims to stretch the limits of Electronic Smart Systems (ESS) in terms of energy autonomy, decision making and maintenance-free lifetime extension as well as miniaturization, by applying a high aspect ratio design architecture. The ultimate goal of the project is to develop and validate a cost-attractive next generation ASSC that will be used in IoT applications for smart living and working environments. Three versions of the ASSC are anticipated: an indoor, an outdoor and a wearable version. The ASSC will be tested and validated for various use case scenarios in the context of smart cities, smart homes and industrial environments. More specifically, use case scenarios may include air quality monitoring through fleets of vehicles, asset tracking and surveillance of objects, people detection, indoor comfort and air quality, indoor occupancy and productivity, health, safety and environmental monitoring during inspection activities. The complete use case scenarios of AMANDA will be reported as part of **Deliverable D1.3 – Voice-of-the Customer completed**, due on M5 of the project.

The ASSC's energy autonomy booster, connectivity and tracking subsystem, processing unit, multi-sensing adaptable sub-system and the encapsulation and packaging sub-system will enhance the partners' technological excellence. Security by design mechanisms will also be employed to ensure minimum vulnerability, user and device authentication, intrusion prevention and detection as well as an overall enhanced cyber-secure operation.

The sensors that will be developed by the AMANDA Partners for the ASSC under Tasks **T2.1, T2.3 and T2.5** are the following:

Sensors	
CO_2 sensor (IMEC)	Image sensor (EPEAS)
Capacitive sensor (Microdul)	Temperature sensor (Microdul)

Table 1 List of sensors developed by AMANDA Partners for the ASSC

Additionally, off-the-shelf sensors will be investigated under **Task 2.2**.

2 SoA, Benchmarking and Feasibility study

This Section presents a SoA analysis for different sensors, MCUs, energy harvesters, batteries, power management systems, wireless technologies, packaging and PCB designing. Additionally, a benchmarking analysis of the available solutions in comparison with the Partner-developed sensors or technologies was carried, focusing on the feasibility of the individual components for the ASSC, mainly in terms of required current. For all the parts and components that will be part of the ASSC for the AMANDA project, a full specification is given below.

2.1 Imaging Sensors

Image sensors (or CIS) provide vision capabilities to an object. During the last decade, huge advances have been brought to high-resolution image sensors integrated into smartphones and other devices. These sensors consist of a very large number of pixels and have been granted a drastic noise reduction. On the other hand, they consume large amounts of energy. For IoT and embedded systems, the opposite trend is required: the reduction as much as possible of the power consumption by lowering the resolution and tolerating additional levels of noise.

Research exists on image sensors that work with a very low-power consumption [1] [2] [3] [4]. These CIS feature a very low energy consumption, with under 50pJ/frame/pixel and rely on the reduction of the supply voltage to lower dynamic losses. However, the achievable resolution is very low and does not comply with industry standards such as VGA resolution.

Manufacturer	Array resolution	Supply	Max frame rate	Total power	Energy	Dynamic range	Peak SNR
Omnivision OV7261	640 x 480	Analog: 2.8V I/O: 1.8V	100fps	117mW (@100fps)	3800 [pJ/frame/pixel] @100fps	69.6dB	38dB
Cmosis CMV300	640 x 480	Dual: 1.8V and 3.3V	120fps	700mW	19000 [pJ/frame/pixel] @100fps	60dB up to 90dB with HDR	43dB
On Semi MT9V032	752 x 480	3.3V	60fps	320mW (@60fps)	18600 [pJ/frame/pixel] @100fps	55dB >80-100dB in HDR mode	-
ST VS6502	644 x 484	2.6V to 3.6V	30fps	< 30mA	10500 [pJ/frame/pixel] @100fps	>52dB	37dB
Samsung prototype JSSC2015	640 x 480 320 x 240	0.9V/1.8V/3.3V	15fps	2.28mW (PS) 45.5µW (AO)	500[pJ/frame/pixel] (PS) 34.3 [pJ/frame/pixel] (AO) @15fps	50dB	-
UCLouvain 3rd generation	640 x 480	0.7V	8fps	-	85 [pJ/frame/pixel] @ 8fps	60dB	37.8dB
Rüedi et. al., CSEM,2019 [5]	320 x 320	1.8V	10fps	700µW	683.59 [pJ/frame/pixel] @10fps	120dB	-
Couniot et.al., JSSC, 2015 [6]	128 x 128	0.6V	32fps	8.8µW	17 [pJ/frame/pixel] @32fps	42dB	27dB

Chen et.al., JSSC, 2014 [7]	816 x 640	1.8V	28.7fps	0.72mW	48 [pJ/frame/pixel]	34dB	25dB

Table 2 SoA low power image sensors

Regarding the power consumption reduction, high precision ADCs cannot be used anymore to convert the light information into a digital value as they consume a lot of energy. Hence, one of the main challenges lies in the design of new paradigms of sensors architecture.

Based on previous work from the Université Catholique de Louvain (UCLouvain) [4] [8], EPEAS will develop for the AMANDA project a fourth generation ultra-low power time-based image sensor. These imager sensors convert the light information into a pulse whose length depends on the intensity. The pulses are subsequently converted to a digital value via counters.

For industrial applications, the signal to noise ratio (SNR) and dynamic range (DR) should be increased. Power consumption should also be decreased. The main challenge lies thus in the research of new ways to improve the existing architecture.

2.2 Capacitive Sensors

Capacitive sensing is an established technology employed in a wide range of applications. In particular, it is used in nearly all mobile devices, including smart phones, tablets, smart watches, eBook readers, wearables and toys, but also in a large part of other customer and household electronic devices such as TVs, coffee machines or cookers. The touch-sensitive devices, based on capacitive sensing, are nowadays pervasive. The technology is mostly mature.
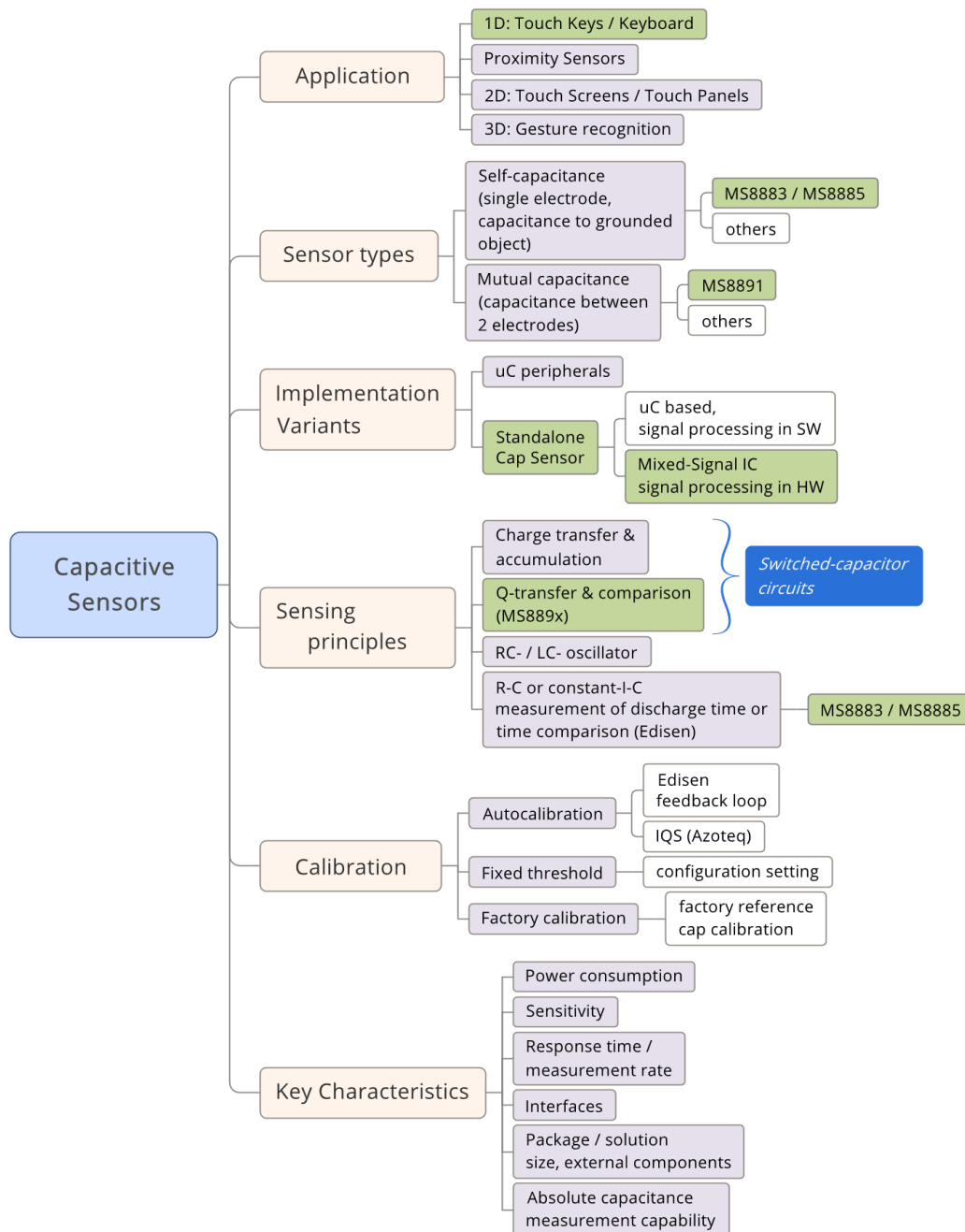
Figure 1 Capacitive sensing overview

A summary on capacitive sensing and its applications is given in [9] and a recent overview of capacitive sensing in human-computer interaction is given in [10].

2.2.1   Application areas

Capacitive sensing is established in several application areas. These can be categorized for instance by their dimensionality:

- *0 and 1-dimensional applications:* Individual sensors and arrangements of multiple individual sensors for touch keys fall in this category. Keyboards and sliders are usually formed from multiple individual touch sensors or from a matrix arrangement of sensors. In a key matrix, two sensors may be combined in one key, which allows reduction

of the number of sensor lines required for a given number of keys: for example, a 16-key panel in 4x4 shape can be formed using 8-sensor channels. Proximity detecting capacitive sensors also fall into the 1-dimensional category. These already react on approaching objects at a certain distance (usually in the 1 to 10 centimetre range). The sensing principles are the same as for the touch key, but the sensors are usually physically larger and the measuring circuit must have an increased sensitivity to capacitance changes.

- *2-dimensional applications:* Touch screens (mobile devices, touch screens on notebooks, point of sales displays, industrial control, etc.) and display-less touch panels (notebooks) fall into the two-dimensional category of capacitive sensors. Capacitive touch screens are normally based on a dense matrix of electrode lines.
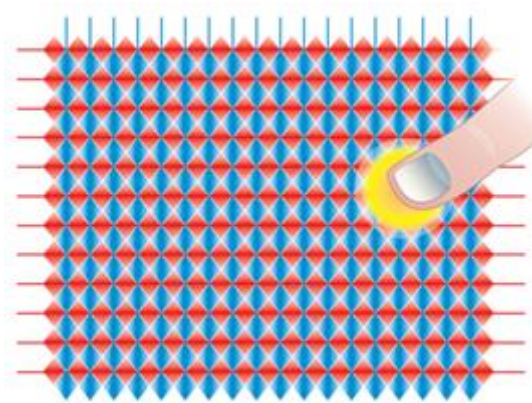
Figure 2 Projected capacitance-based touch screen (taken from [3M, 2013])

- *3-dimensional applications:* Less mature, and not widely seen in the market yet, are capacitive sensing applications able to recognize gestures in 3D space, usually above a touch screen [11]. In the AMANDA project, the role of the capacitive sensor is to provide an ultra-low power switching function, like system wake-up or triggering single functions. For this reason, the SoA analysis concentrates on capacitive switches with single or a few dedicated touch sensors, and leaves the capacitive touch screen technology aside.

2.2.2   Sensor arrangements

Capacitive sensors measure capacitance in two essentially different arrangements, as demonstrated in the following Figures.
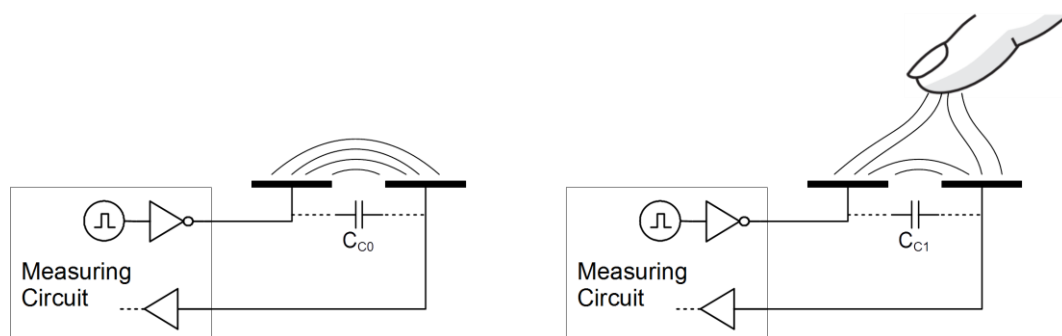
Figure 3 Mutual capacitance arrangement, untouched (left) and touched (right)

In the case of mutual capacitance sensing, as shown in the Figure above, the capacitance between two conducting shapes (electrodes) is detected. One electrode is actively driven with an AC signal. The signal is capacitively coupled (C_{C0}) to the second electrode. The return signal is analysed in the measuring circuit. An approaching or touching object disturbs the electric field between the electrodes and effectively reduces the coupling capacitance between the electrodes, thus $C_{C1} < C_{C0}$. This capacitance change is detected and processed in the measuring circuit.
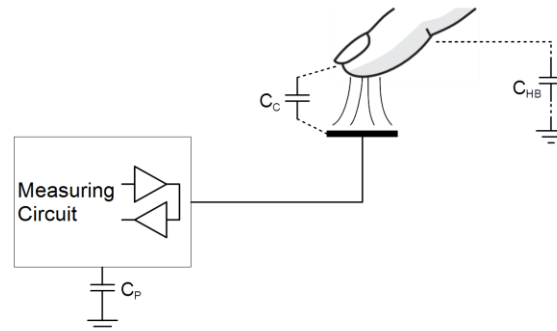
Figure 4 Self-capacitance arrangement

In the case of self-capacitance sensing, as depicted in the Figure above, the coupling capacitance between a single sensor electrode and an approaching or touching object C_C is detected. In most applications, the measurement is performed in two phases: at first, a signal is applied to the electrode. Then, in a second phase, the reaction to the signal is measured. This reaction (amplitude, delay time or another parameter) varies with changes in the sensor capacitance C_C.

In the self-capacitance arrangement, the parasitic capacitances C_P (capacitance of the measuring device to earth) and C_{HB} (capacitance of the human body to earth) have a significant effect on the sensitivity and behaviour of the circuit.

Proximity sensing at distances larger than a few millimetres is usually implemented with a self-capacitance arrangement. Keyboards and touch screens are mostly using the mutual capacitance arrangement.

2.2.3   Application variants

Capacitive sensor measuring functionality is most often applied in one of three different ways:

1. **Standalone function**: The only task of the circuit is capacitive sensing. The sensor IC is usually implemented as a mixed signal circuit with a larger analog section and a small digital control unit, based on a state-machine and a few registers. Often the IC has only a direct switching output and no configurability over a serial interface. Examples of this architecture include the Microdul capacitive switch families MS888x and MS889x.

2. **Standalone function with embedded microcontroller**: Again, the only task of the circuit is capacitive sensing. These circuits however, rely on extensive digital processing to obtain increased sensitivity and/or improvements in noise performance. Usually the devices contain a serial interface and provides a number of configuration registers, but the firmware is hard-coded and cannot be altered by the customer.

3. **Implementation as microcontroller peripherals**: Some of the major players in the microcontroller market developed or acquired capacitive sensing expertise and added capacitive sensing functionality as peripherals into their microcontroller product lines. This approach has the advantage of lower cost, as no additional sensor IC is required, and increased flexibility, as the processing software can be optimized by the user. On

the negative side is the increased power consumption, as the controller has to be running during an active sensing. In addition, software development for the controller is complicated, because the handling of the capacitance measurement must run in parallel to the main application. The microcontroller peripherals often use simple capacitance measurement methods and have limited sensing performance (for example Microchip PIC microcontrollers with Capacitive Voltage Divider, CVD).

2.2.4 Capacitance sensing principles

One of the most widely applied sensing principles is based on charge transfer. In the first phase, the variable capacitance to be measured is charged up to a fixed voltage, for instance up to the supply voltage level. The stored charge $Q = C * V$ is directly proportional to the sensor capacitance. In a second phase, this charge is transferred to an internal or external fixed capacitor that is dependent on the charge and where a voltage is produced. For most cases, the transfer is repeated several times in a burst in order to accumulate more charge and obtain a better measurement resolution.

A multitude of evaluation methods exists to determine the transferred charge and relate it to the sensor capacitance. Among them are:

- The direct **A/D conversion** of the resulting voltage.
- **Counting the number of charge transfer cycles** required to reach the defined voltage level on the integrating capacitor (*Azoteq* ProxSense®).
- One-step **charge comparison** of the transfer charge with a reference charge in a 'charge-comparator' (*Microdul* MS8891). The single charge comparison with an internally generated reference charge allows a touch / no touch decision. The reference charge can be digitally controlled. Optionally, the actual sensor capacitance value can be determined in a successive approximation sequence.
- **Sigma-Delta A/D conversion** principles enable a very high measurement resolution, at the cost of increased power consumption (e.g. *Analog Devices* AD7151).
- In *Cypress*'s CSD technology (CapSense® with Σ-Δ modulator), the sensor capacitance forms one element in a **switched capacitor sigma-delta converter**. Thus, also the Cypress technology is a variant of the charge-transfer principle.
- Also, a major player in the capacitive sensing market for keys, sliders and others is *Microchip* who provides three lines of sensor ICs. The most widespread one, with the largest portfolio, are the AT42QTnnn series of circuits. These are also based on a **burst-mode charge transfer** method. The principle was initially developed by a company called Quantum, which was acquired by Atmel, which in turn was taken over by Microchip recently.

Once the capacitance value has been converted and digitized, an algorithm compares the result with a switching threshold. The threshold may be fixed or automatically adjusted to the environmental changes. The complexity of the digital processing ranges from rather simple state-machines over software implementations in embedded MCU cores to full-fledged DSPs. Besides the most widespread charge-transfer based principles, several other capacitance measurement approaches can be found in the market:

- **R-C and L-C oscillators** using the sensor capacitance as frequency-defining element. The variation of the external sensor capacitance leads to a frequency variation, which can be measured easily when an MCU with a stable clock frequency is available in the system or embedded in the sensor IC.
- **Discharge time comparison** (*Microdul* MS8883, MS8885): The external sensor capacitance and an internal reference capacitor are initially charged to VDD level. The two capacitances are then simultaneously discharged through resistors (R-C discharge). The discharge time difference between the two R-C elements, due to dynamic changes in the sensor capacitance, is captured and evaluated.

2.2.5   Calibration and auto-calibration

The capacitance values of typical sensor arrangements are in the range of a few picofarads (pF) for mutual capacitance electrodes and 10 – 50pF for self-capacitance sensors. The measurement resolution must therefore be in the femtofarad (fF) range. Capacitance variations due to parasitic elements, mechanical tolerances, variations in the permittivity of the involved materials, consistency in the manufacturing of the sensor, accumulation of dirt or humidity, temperature variations and other effects are usually larger than the measurement resolution and can vary over time. This complicates the application of capacitive sensors in applications and may require costly measures in the product design and in the manufacturing processes, like factory calibration of each device. To alleviate this situation, signal-processing features have been introduced in many of the sensor ICs that allow for automatic compensation of manufacturing tolerances and/or slowly changing conditions. These measures are named "auto-calibration", "auto-tuning implementation", "auto-drift-compensation" or otherwise by the different sensor IC suppliers.

Some devices (*Microdul* MS8883, MS8885) implement an auto-calibration feedback loop. The circuit adapts slowly to the actual sensor capacitance. Absolute tolerances and slow changes are compensated. The circuit reacts to dynamic capacitance changes due to a moving or touching object. Other devices implement their auto-calibration methods using digital signal processing of the measured value, including filtering or dynamic threshold setting.

2.2.6   Advances in capacitance sensing and measurement

In the current research, a major focus is on capacitance-to-digital conversion (CDC) for sensing applications in the medical, health care and IOT domains. Several types of sensors, often MEMS based, provide capacitance as a measurable parameter, including: pressure sensors [12] (air pressure, blood pressure, tumour detection), humidity sensors [13], proximity sensors [14], sound pressure sensors [15], [16], or physical force sensors [17]. Capacitance sensing is a preferred principle due to the inherently low-energy requirement as the capacitive sensors don't draw static current.

For power consumption comparison, two FoM are in general use: a) the average power consumption per sensor input at a reasonable measurement rate [18], and b) the energy consumption per conversion-step[1] [19], [20], which is directly dependent on the resolution of the CDC converter. Recently Xin, et.al. described a multi-purpose versatile CDC [21] with the best FoM reported so far, which is suitable for use with a multitude of sensor frontends. The energy consumption per conversion-step reported is ~20fJ/c-s and the average conversion power is directly dependent only on the measured capacitance and ranges from 70nW to 1μW at the fastest sampling speed. These FoM have made significant progress in the recent years and are only possible due to CMOS technology scaling, which provides ever lower capacitance values and allows for lower supply voltages [22], [23].

Capacitive sensing for touch detection is a mature field and has been adopted in the industry since several years. There is little research activity, especially in the area of button touch interfaces. More recent publications exist in the field of sensor optimization for touch panels [24], in 3D gesture sensing [25], [26], or in multi-touch capable panels or screens.

2.2.7   Market situation

The largest suppliers in the marked for capacitive touch sensors (individual touch keys, sliders, wheels) are Cypress, Azoteq and Microchip. Other players include Microdul, Texas Instruments, Semtech, Analog Devices, SiLabs, and a few Chinese manufacturers (Tontek, Ronghe,

---

[1] FoM = $P_M * T_M / 2^{ENOB}$ with P_M = Measurement power, T_M = Measurement time, ENOB = Effective number of bits

AD Semi). Additionally, there are a number of companies that just have a single specialty product in their offering, like EM Microelectronic (EM6420), IDT (Integrated Device Technology, ZSSC3122), AMS (Austria Microsystems, PCap04) or ISSI (Integrated Silicon Solution, IS31SE5100).

It should be noted, that some of the larger companies have already discontinued their lines of capacitive sensors. Such companies include NXP (discontinued the acquired Freescale touch sensor line MPRnnn) or ST Microelectronics (S-Touch line). Other major players like Microchip have acquired smaller companies with a strong capacitive sensing portfolio in order to get into this market.

2.2.8   Key characteristics

Key characteristics of the capacitive touch switches considered in this SoA analysis, in rough order of importance, are:

- **Active power consumption**: in a state where at least one sensor is active
- **Sensitivity**: Sensitivity or measurement resolution is a very difficult to specify parameter, and the different sensor IC suppliers specify it differently or not-at-all. The difficulty comes from the fact that the actual measured capacitance is mostly not of interest and not available as a value. The switching dynamics, the robustness, and the switching distance are the most compelling characteristics to take into consideration for the sensitivity of the device.
- **Supply voltage range**: interestingly a considerable number of sensor IC families still require supply voltages > 2.5V, which can be a considerable drawback when interfacing in systems nowadays.
- **Package size and type**: in order to fit into the small portable electronics devices like mobile phones or in-ear phones the package size is critical – QFN or chip-size-packages are preferred.
- **External components**: some early solutions required one or several external components, mostly large value capacitors for accumulating charge or storing voltages.
- **Available interfaces**: standalone operation is often preferred in single key applications but for devices with multiple channels it is more efficient to read out the sensor state over a serial interface – I2C is the most common one.
- **Capacitance range**: defines the range of sensor capacitance, including parasitic capacitance that the IC can handle. Moreover, it influences the sensor size and length of conducting traces between the IC and the sensor.
- **EMC robustness**: EMC performance is a challenging topic. By nature, all capacitive sensors are exposed to electromagnetic disturbances, their sensor traces often act as antennas. EMC robustness is achieved by analog filtering on the sensor lines and by post-processing the measurement results.

Comparison and ranking among circuits are difficult because of the many parameters involved, which often depend on each other. Power consumption for instance depends on at least:

- The number of sensing inputs
- The sensing rate (measurements per second) with respect to the reaction time
- The required sensitivity
- The robustness (noise filtering algorithm & setting)

The comparison in the Table 3 includes the following devices with touch switching function and low channel count (1 - 4 sensors): *Microdul* MS8883, *Microdul* MS8891, *Analog Devices* AD7142, *Analog Devices* AD7156, *Microchip* AT42QT1010, *Microchip* MTH101, *Microchip* CAP1293, *Azoteq* IQS128, *Cypress* CY8CMBR3102 and *Semtech* SX9500.

Parameter	MS8891	MS8883	Best device	
Active power consumption[2]	950nA	2.5µA	950nA	MS8891
Physical dimensions (application size)	3x3 QFN 1.5x1.0 CSP no external components	3x3 DFN 1.2x0.9 CSP external components	2x3 DFN no external components	CAP1293
Supply voltage range (lower limit)	1.8V	2.5V	1.71V	CY8CMBR3 102
Sensitivity / resolution	1.6fF	12 - 14bit	< 1fF	AD7142
Reaction time (measurement rate)	30ms	64ms	0.3 - 4ms	MS8891[3]

Table 3 Comparison and best-in-class values for the most important parameters

Notably, the critical parameters for the AMANDA project include the lowest possible power consumption together with the smallest physical size.

Concerning both parameters, the Microdul MS8891 is an excellent starting point. It already has the absolute lowest active power consumption in full operation with less than 100ms reaction time. It also provides a small solution footprint and requires no external components except the sensor electrodes, with the option of using a CSP package.

2.3   Temperature Sensors

Temperature measurement is of paramount importance in a multitude of areas. For humans, temperature plays a role 24 hours a day. Most people require a regulated temperature for well-being, which is achieved by a selection of clothing, heating and/or cooling of inside environments (buildings, transport vehicles) and sometimes even outside (outdoor heaters in restaurants). Temperature measurement and control is also omnipresent in commerce (storage of food, and other products), in the industry (control of machinery temperature to prevent overheating, maintaining controlled production conditions), in pharmacy (transport chain monitoring) and others.

Temperature measurement can be realized in several ways. Temperature sensors can be broadly classified into mechanical types (thermometers based on the physical expansion of materials with temperature, bimetallic strips) and electrical types (thermistor, thermocouple, resistor-temperature-detectors). Each of these types can be implemented with a variety of materials or material compositions, which result in widely different properties, like temperature range, linearity, accuracy, construction size, and cost (often rare and expensive materials like platinum are employed).

With the silicon revolution, a new type of sensor has become available, basically for free, on silicon microchips: the silicon bandgap temperature sensor, which is essentially based on the temperature gradient of the silicon diode voltage. In a first approximation, the voltage difference between two forward biased silicon diodes with different current densities has a linear dependence on temperature:

---

[2] Responsive mode < 100ms delay, typical setup.

[3] Microdul MS8891 in permanent measuring mode. Depending on filtering mode, the reaction time varies. Some other devices also reach rates in the single digit millisecond range.

$$VBE \ = \ \frac{kT}{q} \cdot \ ln\left(\frac{ID1}{ID2}\right)$$

Based on this property, the temperature of the silicon diode can be determined. PTAT (Proportional to Absolute Temperature) based circuits utilizing either BJT or CMOS transistors are widely used in nowadays temperature sensors.

Besides the low cost, minuscule size and ready availability of the sensing element on integrated circuits, a further advantage is the availability of electronic processing – analog and/or digital – to increase accuracy of the measurement, to compensate second or higher order non-ideality factor and to provide the result as digital information.

The following SoA overview exclusively covers silicon-based temperature sensors.

2.3.1   Key performance criteria

The most important criteria for silicon temperature sensors are measurement accuracy and power consumption. Secondary parameters are temperature measurement range, measurement resolution, package size, supply voltage range and additional features.

2.3.2   Advances in solid-state temperature sensors

Main advances in accurate solid-state temperature sensors based on the temperature characteristic of the forward biased Si-diode were mostly introduced several years ago [27], [28], [29], [30]. The Microdul temperature sensor for AMANDA will be based on this established sensing principle while further reducing the power consumption to become the best in the market, as detailed in Section 4.3.

More recently, alternative measurement principles have been reported, allowing to reduce the power consumption considerably for systems in the IoT or medical fields, where energy is harvested or comes from very low-capacity batteries. These new principles however come at a loss of accuracy. In [31], a temperature sensor based on a leakage current-based ring oscillator and a frequency counter is presented. Better accuracy is reached in a CMOS gate leakage-based architecture, as presented in [32].

2.3.3   Power consumption

The power consumption of a temperature sensor is composed of the power needed to keep the sensor alive in idle/standby/sleep mode, when no measurement is performed, and the power required during active mode, when measurements are performed. Depending on the application's measurement rate, the ratio of idle to active mode has a major impact on the average power consumption.

In order to obtain comparable figures for the different sensors analysed, the average power consumption per second and per minute, for a single measurement, is extracted from datasheets.

Additionally, influential factors on power consumption are differences in functionality. For example, a sensor that cyclically measures temperature requires an internal oscillator for triggering the measurements. Such a sensor normally consumes more power when it is in an idle mode due to the oscillator.

2.3.4   Accuracy and calibration

Accuracy is directly related to the temperature range over which the accuracy is reached. Often the accuracy is best over a limited temperature range (usually around the calibration point), and the accuracy is reduced over the full temperature range.

Analog integrated circuits are built from a number of components, like resistors (polysilicon or diffusion resistors), capacitors, transistors (MOS or bipolar) and diodes. The properties of these components usually have a considerable process variation from device to device and from lot to lot, but they also have temperature and voltage dependencies. Parameters often

vary by 20% or more. The same holds for the derived voltages and currents. Circuit architecture and design often allow compensating for such variations to a certain degree, and functions can be made tolerant to variations.

For temperature sensing, a high absolute accuracy is demanded. This usually requires a calibration or adjustment step. The sensors in most cases embed non-volatile memory to hold calibration information. Calibration per device is a complex step in the manufacturing process. This is a wide field of expertise that is assembled by each manufacturer. Calibration can be performed at a single temperature point or at multiple points. Calibration can be done on wafer level or with the packaged device. The trade-off between achievable accuracy and cost per device is essential. Microdul aims to keep cost low with a one-point (one temperature) calibration at wafer level.

Accuracy is also related to other parameters indirectly. Accuracy can be increased by spending more power for example by using higher currents in analog blocks or performing multiple measurement cycles combined with averaging.

2.3.5   Other parameters

Packaging: Most SoA solid-state temperature sensors are available either in encapsulated plastic packages of the QFN type or in CSP. QFN and similar plastic packages have the advantage of easy application in PCB assembly. On the other hand, they may have reduced accuracy if the calibration was on a wafer level, and they have worse heat transfer properties which can also manifest in reduced accuracy. CSP package in turn leads to the smallest possible solution footprint, but is more challenging in the application because the silicon die is exposed and light influence can affect the performance and / or power consumption.

2.3.6   Additional features

Besides the core function of temperature measurement, the temperature sensors can be differentiated by additional peripheral functions, like:

- **Interface choice**: the most common interface is I2C for sensors with digital outputs, but SPI is also employed and less frequently analog DC voltage output, analog voltage output in PWM format. The *Microdul* MS1088 additionally features a digital handshaking feature: measurements can be triggered by pulling a digital handshake line low for a short time, and after the completion of the measurement, the MS1088 indicates this by pulling the handshake line down in its turn. This feature allows the controller to sleep during the measurement instead of polling for the result.
- **Autonomous measurements**: Some devices (*AMS* AS6200) implement autonomous cyclic measurements combined with the check of a warning threshold.
- **Temperature monitoring**: Temperature monitors are specialized temperature sensors, which cyclically measure temperature, compare the result with one or several temperature thresholds and record the excursions in memory. In case of exceeding a limit criterion, they can set and display an alarm state. Temperature monitors are often employed stand-alone without an attached microcontroller.

Accuracy comparison between devices is complicated by the fact that accuracy definitions are always related to a temperature range over which they are valid. Often the accuracy is better over a narrow temperature range around room temperature. Some sensors are optimized to work best in a narrow temperature range around the human body temperature.

For this reason, three temperature ranges have been defined in the following comparison and the accuracy for each device is estimated from the datasheet specifications that may have needed some interpolation.

Parameter	MS1088 Microdul	TMP117 TI	AS6200 AMS	STS35 Sensirion	Si7053 SiLabs
I_{active} [μA][4]	75	135	50	600	90
I_{idle} [nA]	20	150	100[5]	200	60 (620 @ 85°C)
$I_{1\,Hz}$ [μA]	4.1	3.5 - 16	1.5	1.7	0.27
$I_{1/60\,Hz}$ [nA][6]	80	210	130 (40)[7]	225	63
t_{conv} [ms]	50	16	32	2.5	2.4
E_{unit} [μJ][8]	11.25	7.1	4.8	5.0	0.72
$A_{10/40}$ [°C][9]	0.3 / 0.5	0.1	0.4	0.1 typical 20 ~ 60 °C	-
$A_{-20/85}$ [°C][10]	-	< 0.2	-	0.3 max -40 ~ 90 °C	-
$A_{-40/120}$ [°C][11]	1.5 / 2.0	< 0.3	1.0	0.6 max -40 ~125 °C	0.3 max -40 ~125 °C
V_{sup} [V]	2.4 - 3.5	1.8 - 5.5	1.8 - 3.6	2.4 - 5.5	1.9 - 3.6
Package type & size [mm]	QFN 16 3 x 3	WSON 6 2 x 2	CSP 6 1.5 x 1.0	DFN 8 2.5 x 2.5	DFN 6 3 x 3
2nd package type & size [mm]	CSP 12 1.39 x 0.93	-	-	-	-
Price [$][12] @1k	-	2.99 (Arrow)	0.81 (Digikey)	1.25 (Digikey)	1.45 (Arrow)

Table 4 Direct comparison of a few SoA temperature sensors

---

[4] Current consumption during actual measurement process

[5] Oscillator running in external triggered mode; the standby current could be as low as $10 nA$

[6] Calculated from idle current, active current and conversion time ($I = Iidle + Iactive * tconv / 60s$)

[7] 130nA theoretical value, not practically reachable as 1 measurement/minute is not a valid mode. Sleep current is not specified, but assuming $Isleep = 10nA$ the single conversion ever minute current $I1/60Hz$ becomes about $30nA$

[8] Energy required per measurement at the best accuracy level and at the nominal supply voltage:

$$EUnit = Vdd * IActive * tConv$$

[9] Accuracy values are always maximum values over the specified range, unless otherwise noted

[10] as above

[11] as above

[12] Lowest distributor price at 1k, search through findchips.com

Parameters in the Table 4 are typical values from datasheets, unless otherwise noted.

2.4   CO₂ Sensors

CO_2 sensing can be accomplished in several ways, but most commonly with optical and electrochemical methods. Infrared light absorption sensors usually are power hungry and bulky. Those features come from the fact that light needs to be emitted by a bright source such as LED lights and that the optical measurement channel needs to be long enough for the optical absorption to be registered.

One example of a SoA optical sensor currently on the market is the *COZIR* GC-0011 [33]. The dimensions of the sensor are depicted in Figure 5. Its power usage peaks at 33mA and on average is <1.5mA at 3.3V supply voltage. The data output is done by a UART interface that uses a calibrated value.
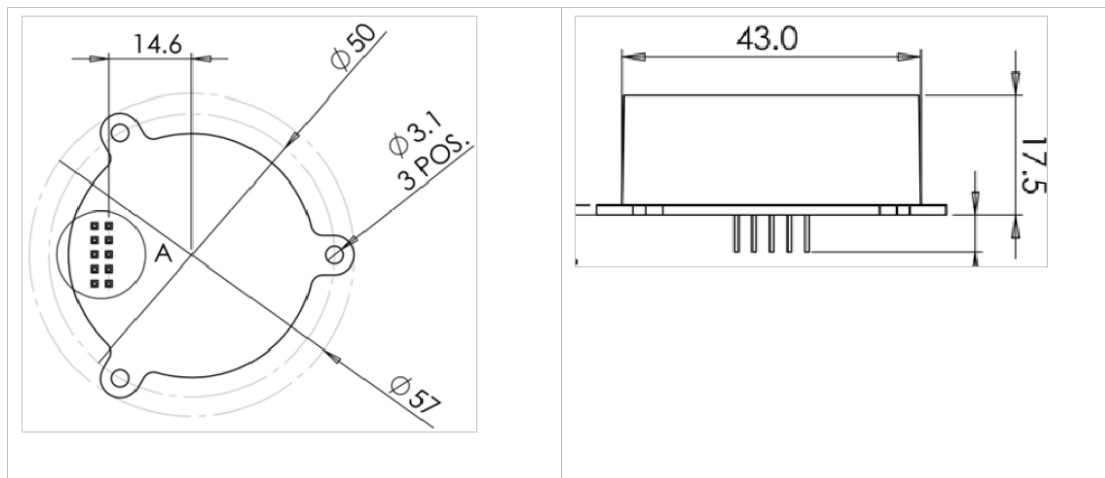
Figure 5 Dimensions of the COZIR GC-0011 CO_2 sensor [33]

Model	CO₂	DS-0147 [34]	LP8 [35]	T6713-EP [36]	SCD30 [37]	GC-0010 [38]
Manufacturer	IMEC	ExplorIR	SenseAir	Telaire	Sensirion	COZIR
Supply Voltage	2.8V – 3.6V	3.25V - 5.5V	2.9V - 5.5V	4.5V - 5.5V	3.3 V - 5.5 V	3.25V - 5.5V
Current	2mA Idle 30mA peak	1.5mA average 33mA peak	31-225µA average 125mA peak	25mA average 200mA peak	19mA average 75mA peak	1.5mA average 33mA peak
Power Consumption	-	3.5mW (2Hz)	-	-	-	3.5mW (2Hz)
Sensing Method	Printed ionic liquids on semiconductor surfaces	Non-dispersive infrared (NDIR)	NDIR	NDIR	NDIR	NDIR

Response Time/Period	500ms	10s - 2 mins	≥ 16s	< 3 mins	20s	30s - 3 mins
Dimensions	10 x 5 x 1mm	20 x 20 x 21mm	8 x 33 x 20mm	30 x 15.6 x 8.6mm	35 x 23 x 7mm	57 x 57 x 17.5mm

Table 5 Off-the-shelf CO_2 sensors benchmarking

2.4.1 SoA electrochemical sensors

The level of CO_2 in the atmosphere can also be measured by electrochemical sensors. The CO_2 sensitive element consists of a solid electrolyte formed between two electrodes, together with a printed heater (RuO_2) substrate. It is possible to measure the CO_2 gas concentration by monitoring the change in the electromotive force (EMF) generated between the two electrodes [39]. An example of an electrochemical sensor available in the market, is the FIGARO TGS 4161.
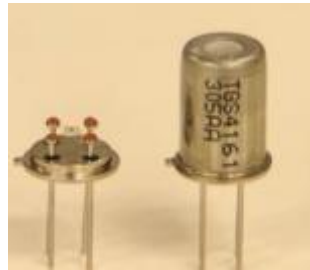
Figure 6 The Figaro TGS4161 CO_2 sensor [39]

Figure 6 depicts the TGS4161 transducer. The component dimensions are 9.2x14.2mm. A disadvantage of the transducer is its analog nature, requiring thus additional electronic circuitry as well as an analog to digital converter in order to provide digital data. This results in an increased size for the component. In order to function properly, the sensor also requires heating, which increases its power consumption significantly.

According to the specifications, the sensor operates with a power supply of 5V with an average consumption of 50mA [39].

Since the beginning of the AMANDA project, there have been some developments in the SoA for CO_2 sensors. From an academic point of view, there seems to be little interest in developing new sensors or sensing mechanisms for gas sensing. While there are some papers on the use of thermal conductivity measurements to sense changes in gas composition [40], [41], [42], the high cross-sensitivities towards fluctuations in barometric pressure, humidity and temperature make them unsuitable for non-controlled environments with multiple components as we have both indoors and outdoors.

There have been some developments in the commercial field though. Both Infineon (XENSIV PAS210) [43] and Sensirion (SCD40) [44] have presented a CO_2 sensor which is also NDIR based as most sensors on the market, but where the signal detection is performed by using a photoacoustic effect. Compared to current sensors which work by using filters and optical detectors, the switch to photoacoustic detection makes it possible to further simplify the sensor setup. By implementing cheap and well-known MEMS microphones, both suppliers claim to have the smallest sensor on the market with devices the size of sugar cubes. First price indications are in the range of 10-20 dollars per device on a large scale, making it very attractive for many air-quality-related applications. The official launch of these sensors is planned for 2020 and additional information on e.g. power consumption or sensitivity is scarce. The height of these sensors is listed as 7mm (for the Sensirion model) which unfortunately makes them unsuitable for use within the AMANDA project.

2.4.2   IMEC Carbon Dioxide Sensor

The IMEC carbon dioxide sensor consists of an analog parametric transducer and an integrated circuitry that is able to convert a change in impedance to a CO_2 concentration value. The sensor itself consists of a silicon die covered with a thin layer of non-volatile electrolyte on platinum electrodes. The measured CO_2 interacts with the electrolyte and changes its properties. These changes can subsequently be monitored, by measuring the electrical impedance between the electrodes. Currently, the active area of the sensor is 4x4mm. By including bond pads, the die area is slightly larger. It is possible to decrease the size further by using a different design of electrodes but the effects on the sensor performance are not yet known. This research activity will be performed during the AMANDA project.

As described, the IMEC electrochemical CO_2 transducer changes the impedance depending on the CO_2 concentration. The electrical impedance needs to be read out and be converted to a digital value. Routinely, these measurements are carried out by using big and expensive hardware such as potentiostats. This technology became available in a miniaturized form as an integrated programmable circuit in the past few years. The ADuCM350 chip has an integrated analog interface and can be used as a network analyser. It is available in a 120-lead, 8x8mm CSP_BGA package [45]. It only requires an additional oscillator (2x3mm) and a few passive SMD components to operate. It is expected that the readout and the sensor can be integrated in a PCB area of approximately 15x17mm when using double-sided components' placement, without exceeding a height of 3mm.

Figure 7 ADUCM350 microcontroller with essential components, size 15x17mm

Figure 7 depicts the un-optimized implementation of the circuitry needed for the IMEC CO_2 sensor readout. Its area of 15x17mm can possibly be further miniaturized during the development of the AMANDA project.

The IMEC CO_2 transducer is a passive component that can operate at a room temperature. It needs to be electrically excited by the readout circuitry. Even though the electrochemical transducer itself does not need to be directly powered, the readout circuitry needs to be powered. It is estimated that a measurement takes about 500ms. During this time, the current consumption of the readout is about 20mA. The readout operates with a flexible voltage between 2.2V and 3.4V. After the measurement is done, the system can be completely turned off by an external switch, or can be set in a low power sleep mode. The readout can provide the digital data via a UART interface.

As described above, there is no device available on the market that would fulfil the requirements of size and power consumption demanded by an autonomous system in the size of a credit card. That is why that the low power, low profile IMEC CO_2 sensor is the only CO_2 sensor that is suitable to be used in the project.

2.5   MCUs

This Section compares the MCUs that consume the least power and are available currently on the market, or will be available in the near future.

2.5.1   Power consumption and processing power

Low power MCUs generally implement two types of modes:

- Active mode, where the MCU core is running. In active mode, the consumption varies according to multiple parameters like source voltage, clock speed, activated peripherals and others.
- Sleep mode, where the MCU core is shut down and only a few peripherals are still running. The power consumption will depend on the peripherals that are active, such as memory retention, timers, UART, SPI, and others. More active peripherals in sleep mode mean more possible interactions between the "sleeping" MCU and its environment, but it also means more power consumption during that mode.

Those low power modes are not optimized the same way for each device. It depends instead on the target application. Some of them are made to be active most of the time while others are more focused on sleep modes with a very low power consumption. There is no such thing as a "one size fits all" MCU, and the application must always be considered before choosing the most appropriate one.

In low power systems, where minimizing the consumption is extremely important, the code must be thoroughly conceived to make the MCU be active only for useful processing operations. As soon as those operations are done, the MCU should go back to a sleep mode, waiting for the next event to be processed.

Generally, the consumption of a microcontroller is directly related to its processing power, but a powerful microcontroller runs faster, and thus will be active during a shorter period of time to make the same process than a slower one. So, the MCU must be carefully chosen considering the application.

2.5.2   MCU comparison

The Cortex ARM MCUs have an architecture designed specifically for low power consumption. Table 6 below compares technical characteristics of different MCUs, including the CoreMark benchmark that measures their performance in terms of the raw power of their CPU. Note that EDMS M0 refers to a general-purpose microcontroller series from EPEAS.

Model	Bits	ARM Cortex	CoreMark [#/MHz]	F. Max [MHz]	Flash [KB]	SRAM [KB]	Active [µA/MHz]	Passive [µA]
EDMS M0	32	M0	2.33	24	256	32	29	0.75
SAM L10/L11	32	M23	2.62	32	64	16	25	0.5
SAM L21	32	M0+	2.46	48	256	32+8LP	67	0.48
KL03	32	M0+	2.46	48	32	2	114	1.47
EFM32ZG	32	M0+	2.42	24	32	4	114	0.5
STM32L071	32	M0+	2.35	32	192	20	93	0.86
STM32L496	32	M4	3.42	80	1024	320	37	0.48
STM32L562	32	M33	3.88	110	512	256	60	3.6
STM32H753	32	M7	5	400	2048	1024	180	2.6
MSP432P401R	32	M4F	3.41	48	256	64	80	0.64

ADUCM4050	32	M4F	-	52	512	128	41	0.78
RL78/G14	16	-	0.89	32	512	48	66	0.23
Apollo1	32	M4F	3.4	24	512	64	35	0.42
Apollo2	32	M4	3.4	48	1024	256	13.6	3.2
Apollo3	32	M4	3.4	96	1024	384	27	2.7
GAP8	-	-	3.19	170	0	576	80	2

Table 6 Low power MCU comparison

Many processors on the market claim to be low power. Since all these claims cannot be veri-fied, the AMANDA project relies instead on the EEMBC results [46] and on the experience and measurements of the project's Partners while using some of the devices. The EEMBC calcu-lates the energy efficiency of a device when it runs some basic tasks often found in embedded systems. Some of the devices that currently show the best EEMBC scores in terms of CPU performance when energy consumption is taken into account are listed in the following Table, with the addition of some features considered important for the AMANDA project, such as the memory size or the package type. Where appropriate, Partners' experience is included, regarding the quality of support, the energy requirements as well as other characteristics.

Device/firm Memories	EEMBC CP/PP score	Packages	V_{dd}: Min Max	Currents/others	Remarks
RSL10[13] (Cortex M3) On Semi 384kB Flash 76kB Program Memory 88kB Data Memory	1090 @ 3V 1260 @ 2.1V na na	5.50mm^2 WLCSP 6 x 6mm QFN	1.1 3.3	@(1.25V VBAT): Deep Sleep, IO Wake–up: 50nA Deep Sleep with 8 kB RAM Retention: 300nA. This device has also been measured by ZHAW Energy: It is (one of) the best BT Smart SoCs	Includes BLE transceiver (radio has 802.15.4 features). Support for 802.15.4 is to be checked Support has been ok for ZHAW
RSL10 + components SIP version[14]	As above	SIP: max 1.56mm thick	1.1 3.3	As above	SIP. Several system components (+ antenna) already integrated.
Apollo 1,2,3 (Ctx M4) Ambiq [15] 512KBR (A3)	395 @ 3V 553 @ 2.2V 33 @ 3V 54.8 @ 2.2V	-	-	There are several variations with different memory sizes and sleep current. See Apollo table below for more infor-mation. Apollo3 Blue: needs less energy than the Apollo1 and Apollo2 (3mA for Tx and Rx) Apollo2/Apollo2 Blue have been tested by ZHAW in a research project. Very good en-ergy performance	Apollo1/2 have no transceiver (BLE transceiver available for Apollo2 Blue and Apollo3 Blue) Support from Ambiq has proved rather difficult for ZHAW
ATSAML11E16A VB (Cortex M23) Microchip	280 @ 3V 410 @ 1.8V 118 @ 3V 167 @ 1.8V	-	-	We did not look at more details since there is no special reason to take this device. It has no transceiver and we already have the EPEAS device as master processor	No transceiver
STM32L552 V1 (Cortex M33)	267 @ 3V 402 @ 1.8V	-	-	We did not look at more details since there is no special reason to take this device. It	No transceiver

---

[13] RSL10 information: https://www.onsemi.com/PowerSolutions/product.do?id=RSL10

[14] RSL10 SiP: https://www.onsemi.com/pub/Collateral/RSL10SIP-D.PDF

[15] https://ambiqmicro.com/mcu/

ST	33.5 @ 3V 59.5 @ 1.8V			has no transceiver and we already have the EPEAS device as master processor	
STM32L433RC-P (Cortex M4) ST	264 @ 3V 298 @ 2.2V 107 @ 3V 117 @ 2.2V	-	-	We did not look at more details since there is no special reason to take this device. It has no transceiver and we already have the EPEAS device as master processor	No transceiver
Best Cortex M0 SAML21J18A-UES Cortex M0+ (Microchip) Up to 256kB Flash Up to 44kB RAM	196 @ 3V na na na	64pin TQFP, QFN 48pin TQFP, QFN 32pin TQFP, QFN	3.63 1.62	No specific advantage This device is only listed to serve as reference for the EPEAS device that is also a cortex M0 processor	Max freq. 48MHz CCL, RTC, WDC, AES, TRNG, Several SPI, I2C, USB LIN slave Comparators, ADC, ADC, OpAMP No transceiver
Special devices worth considering (include several wireless possibilities)					
Nordic nRF52811 64 MHz Cortex M4 (Nordic) 192KB Flash 24KB RAM	215 [16] na na na	QFN48,32 GPIOs QFN32,17 GPIOs WLCSP32 15 GPIOs	1.7V 3.6V LDO, DC/DC	0.3 µA in System OFF, no RAM retention 0.5 µA in System OFF, full RAM retention 0.6 µA in System ON, no RAM retention 0.8 µA in System ON, full RAM retention 1.1 µA in System ON, full RAM retention, RTC 4.6 mA at 0dBm TX power 4.6 mA in RX at 1Mbps 5.2 mA in RX at 2Mbps	Bluetooth 5.1, 802.15.4 SPI, TWI, UART, PWM, QDEC, PDM, ADC 128-bit AES CCM, ECB, AAR AoA, AoD features (BT 5.1) 802.15.4 SW available in other devices of the family Very good support of Nordic devices (experience of ZHAW)

---

[16] 215 CoreMark for nRF42 devices of Nordic. Data taken from DS. Not sure if certified by EEMBC. V_{DD} unsure

Nordic nRF52810 [17]				Similar in many things to the nRF52811 This device has been tested by ZHAW. Starts very fast with little energy	Like Nordic nRF52811. But only Bluetooth (no 802.15.4)
ST with LoRa	-	-	-	No official information from ST so far	Cortex Mx and LoRa on one die.

Table 7 Additional MCU comparison

---

[17] https://www.nordicsemi.com/Products/Low-power-short-range-wireless/nRF52811

			1 – 25 of 86						next »

Clear	Hardware	Vendor Score	Cert.	Prod. Si	Core	Compiler	Retention RAM	Ext. DC/DC	Core Profile (3.0 V)↓	Core Profile (User)	Periph. Profile (3.0 V)	Periph. Profile (User)	Date
☐	ON Semiconductor RSL10 Rev 1.0	✓	✓	✓	ARM Cortex-M3	IAR C/C++ Compiler for ARM 8.20.1.14183	8 KB		1090	1260 2.1V			2018-02-08
☐	Ambiq Micro APOLLO512-KBR Rev.A3				Cortex-M4	ARM GCC 4.8.3 20140228	8 KB		395	553 2.2V	33.0	54.8 2.2V	2017-09-11
☐	Ambiq Micro APOLLO512-KBR Rev.A3	✓	✓	✓	Cortex-M4	ARM GCC 4.8.3 20140228	8 KB		378				2015-11-07
☐	Ambiq Micro APOLLO512-KBR Rev.A4			✓	Cortex-M4	ARM GCC 4.8.3 20140228	8 KB		353	490 2.2V	29.4	48.4 2.2V	2017-09-08
☐	Ambiq Micro APOLLO512-KBR Rev.A4 + 32KB SRAM retention			✓	Cortex-M4	ARM GCC 4.8.3 20140228	32 KB		302	384 2.2V	28.2	48.0 2.2V	2017-09-08
☐	Microchip Technology ATSAML11E16A rev B	✓	✓		ARM Cortex-M23	IAR C/C++ Compiler for ARM 8.22.1.15669	4 KB		282	400 1.8V			2018-04-10
☐	Microchip Technology ATSAML10E16A rev B	✓	✓		ARM Cortex-M23	IAR C/C++ Compiler for	4 KB		281	405 1.8V			2018-04-10

Figure 8 EEMBC comparison [46]

	Apollo Lite	Apollo	Apollo2	Apollo2 Blue	Apollo3 Blue
MCU Frequency	24MHz	24MHz	48 MHz	48MHz	48MHz TurboSPOT™ 96MHz
MCU	32-bit ARM Cortex-M4F	32-bit ARM Cortex-M4F	32-bit ARM Cortex-M4F	32-bit ARM Cortex-M4F	32-bit ARM Cortex-M4F DMA
MCU Power Efficiency	34 uA/MHz	34 uA/MHz	10uA/MHz	10uA/MHz	6 uA/MHz
Flash/SRAM	256KB/32KB	512KB/64KB	1MB/256KB	1MB/256KB	1MB/384KB
Voltage	2.2 - 3.8V	2.2 - 3.8V	1.8 - 3.6V	1.95 - 3.6V	1.8 – 3.6V
ADC	10 bit, 13-channel, up to 800 kSps	10 bit, 13-channel, up to 800 kSps	14 bit, 15-channel, up to 1.2 MSps	14 bit, 15-channel, up to 1.2 MSps	14 bit, 15-channel, up to 1.2 MSps
I/O	I^2C/SPI master I^2C/SPI slave UART (1)	I^2C/SPI master I^2C/SPI slave UART (1)	I^2C/SPI master (6x) I^2C/SPI slave UARTS (2)	I^2C/SPI masters (4x) I^2C/SPI slave UARTS (2)	I^2C/SPI master (6x) I^2C/SPI slave UARTS (2)
I²S	-	-	I2S slave for PDM Audio Pass-through	I2S slave for PDM Audio Pass-through	I2S slave for PDM Audio Pass-through
PDM	-	-	Dual Interface for Mono and Stereo Audio Microphones	Dual Interface for Mono and Stereo Audio Microphones	Dual Interface for Mono and Stereo Audio Microphones
Wireless Connectivity	-	-	-	BLE 5 w/ Dedicated Processor	BLE 5 w/ Dedicated Processor
RF Sensitivity	-	-	-	-95dBm	-95dBm
RF TX Max	-	-	-	+5dBm	+4dBm
RX current	-	-	-	3.5mA	3 mA
TX current	-	-	-	5.05mA @ 0dBm 8mA @ +5dBm	3 mA @ 0dBm
Packages	- 2.49 x 2.90 mm 41-pin CSP w/ 27 GPIO - 4.5 x 4.5 mm 64-pin BGA w/ 50 GPIO	- 2.49 x 2.90 mm 41-pin CSP w/ 27 GPIO - 4.5 x 4.5 mm 64-pin BGA w/ 50 GPIO	- 2.5 x 2.5 mm 49-pin CSP w/ 34 GPIO - 4.5 x 4.5 mm 64-pin BGA w/ 50 GPIO	4 x 4 x 0.9 mm 64-pin LGA with up to 31 GPIO	3.3 x 3.2 mm 65-pin CSP w/ 37 GPIO 5 x 5 mm 81-pin BGA w/ 50 GPIO

Figure 9 Apollo MCUs and some of their characteristics (from Ambiq)

2.6   Energy Harvesting, Batteries and Power Management

2.6.1   Energy Harvesting

Energy harvesting has been used for decades for solar panels or bicycle dynamos, but the technology is living a revolution the past few years with applications that vary from industry automations to smart city applications. This is why the development within the Internet of Things (IoT) domain is trying to take advantage of it [47].

Due to the advancement in the energy harvesting field, AMANDA's energy harvester will need to compete with technologies that can be combined with low-power electronics and storage to provide a complete energy harvesting solution. Some of the competition is presented below:

Manufacturer	Total size	Open circuit voltage	Operating voltage	Operating Current	Operating Power	Technology Used	Light Operation Range
EnOcean ECS 300 [48]	35.0×12.8×1.1mm	4V	3V	4.5µA	13.5µW	Amorphous Silicon Solar Cell	200 lux
EnOcean ECS 310 [48]	50.0×20.0×1.1mm	4V	3V	11µA	33µW	Amorphous Silicon Solar Cell	200 lux
Panasonic AM-1606C-MEL [49]	15×15×0.7mm	3.6V	2.6V	3.1µA	8.06µW	Amorphous Silicon Solar Cell	50 -1000 lux
Panasonic AM-1456CA [50]	25x10x0.6mm	2.4V	1.4V	5.3µA	7.42µW	Amorphous Silicon Solar Cell	50 -1000 lux
Eight19 OPV (200 lux) [51]	65x110x0.8mm	2.6V	1.6V	32µA	5.12µW	Organic Photovoltaic	200 – 1000 lux
Eight19 OPV (1000 lux) [51]	65x110x0.8mm	3.3V	2.3V	180µA	414µW	Organic Photovoltaic	200 – 1000 lux
GCell DSSC module [52]	200x150x4mm	5.8V	5.5V	120mA	660mW	DSSC	1000 lux

Table 8 Energy Harvesters: Total size, V_{oc}, Operating Voltage

The main customer and industry pain point is the current need to either have a power-wire (unpractical) or to replace (or manually recharge) the batteries in IoT sensors, devices and products. Battery replacement involves labour, transport and chemical waste that have detrimental environmental impact (increase of CO_2 emissions) and financial consequences (increased Cost-Of-Ownership due to extra maintenance). Energy harvesting can be combined with low-power electronics circuitry and storage to provide a complete energy harvesting solution [53]. It is ultimately required for all use cases requiring sensing, information-storage or transmission.

Currently, there is no Energy Harvesting solution that is capable of being manufactured and can provide the required combination of performance (especially in a low light indoor environment), small size and low-cost for the billions of connected sensors that will be deployed. The closest commercially available Photovoltaic Energy Harvesting alternatives are based on large Silicon material (cm^2-m^2 range) which has much lower efficiency (especially indoors) and cannot fit into space-constrained sensing applications.

Amorphous (a-Si) [54] or Crystalline (c-Si) Silicon provide 3-6µW/cm^2 under typical indoor lighting conditions (200 lux), corresponding to an efficiency of 5-10% indoors which is insufficient for most wireless sensors. They also present a blueish (c-Si) or brownish colour (a-Si) caused by insufficient visible light absorption and unwanted reflections.
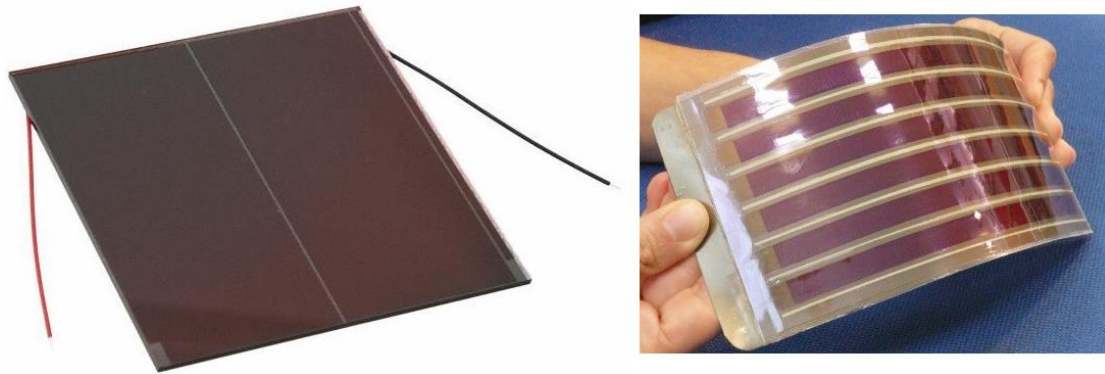
Figure 10 A-Silicon Energy PV Harvester (Panasonic) (left) DSSC Energy harvester (Gcell) (right)

Dye-sensitized solar cells (DSSC), perovskites [55] and organic Photovoltaics (OPV) [56] offer a small power density increase ($\sim$7μW/cm^2 at 200 lux) and can be made flexible. However, they are larger in size (tens of cm^2) and suffer from material degradation and limited lifetime (a few years only). To achieve a smaller footprint, some companies like Solchip are using Complementary Metal-Oxide-semiconductor (CMOS) technology but their power density is too small for most indoor IoT applications.

Aside from commercially available photovoltaic energy harvesters, academic research has been proficient in the field of light energy harvesting, often achieving higher performance than commercial PV cells. Most of the activity appears to be currently focusing on perovskite materials that show good promise for use in indoor environment, and to lesser extent on DSSC and organic solar cells. We recap in the table A below the most noticeable academic results. It is usually difficult to compare results from various laboratories: due to the current lack of measurement standards for indoor solar cells, they are often characterised under different test conditions (different illumination level, spectra, temperature, etc...).

University/Research organisation	Technology	Performance	Comments
University of Swansea (UK) 2018 [57]	Perovskite	16.3-19.9μW cm^{-2} @200 lux	Light spectrum not indicated. Scalability issue for highest performance result
RCNPV (Taiwan) 2019 [58]	Perovskite	11.7%-23.7% indoors	Performance greatly depending on solar cell area
Linköping (Sweden)/Beijing University (China) 2019 [59]	Organic	26.1% @1000 lux	Performance greatly depending on illumination level (worse at low light level)
EPFL (Switzerland) [60]	DSSC	27.5% @200 lux	Performance measured based on photoactive area (not total area). Increases with light level

Table 9 Academic results on best indoor photovoltaic energy harvesters

A general description of advantages and disadvantages of each technology and the main companies is presented in the Table below: most of these technologies are well below 10% efficiency under weak indoor light.

Cell technology	Advantages	Disadvantages

<u>a-Si</u> e.g. EnOcean Sanyo (Panasonic Amorton)	• Cheap (<0.1$/cm^2) • Longer lifetime (up to ~10 years) than DSCCs and OPV • Good overall stability (aside from Staebler–Wronski effect) • Sufficient performance (~5% efficiency at >200 lux) for many simple sensing applications • Can be made flexible (but not generally available as such)	• Very poor performance at <100 lux and not particularly good at <200 lux • Low efficiency means a greater surface area of cells. • Unable to supply sufficient power for more demanding applications even in good lighting (200 lux) • Degradation of efficiency with long term exposure to direct sunlight (Staebler–Wronski effect) • Difficult to make very small (<1cm^2) with existing manufacturing process
<u>DSSC and Perovskites</u> e.g. G24 Power Fujikura	• Efficiencies of 5-15% indoor • Tolerant of polarized light • Better performance at low light levels than a-Si i.e. more linear drop in power with reduced lux • Good performance with low angle of incidence • Can be made flexible	• Limited lifetime (around 5-10 years) • Higher cost than Silicon in the short to medium term • Suitable low-cost barrier layers are still a challenge • Efficiencies not demonstrated in production • Voltage appears to drop off very rapidly below 50 lux • Large surface area typically required (>20cm^2) and lower Open-circuit Voltage V_{oc} (0.58V at 200 lux)
<u>OPV</u> e.g. Eight19	• Potential to be low cost with volume – easily printed in wide areas • Flexible • Low cost substrates e.g. polyester • Translucent • Color tuning • Thin, light weight • Ease of integration into devices • Efficiency advantages over a-Si at very low light levels (up to 50% extra at <200 lux) • Low temperature process • No exotic, rare or toxic materials required • Possibilities for tandem architecture to harvest IR or short wavelength	• Lifetime around 2-3 years with flexible encapsulations and 5-10 years in glass • Suitable low-cost barrier layers are still a challenge • Higher cost than Silicon in the short to medium term • Efficiencies in labs 5-10% and not expected to exceed this for several years • roll to roll produced cells – efficiency ~4% • Low power of approximately 3-4 microwatts/cm^2 at 200 lux and negligible below 50 lux • V_{oc} drops significantly below 200 lux • At best pilot lines but can produce modules

Table 10 Comparison and best-in-class values for the most important parameters

As a comparison, Lightricity uses a high purity and ultra-long lifetime (>20 years) III-V material that delivers over 22μW/cm^2 under the same conditions, corresponding to 30-35% under artificial lights (indoor Fluorescent, white LED, High pressure sodium lamps (parking, outdoor street lights. It can also be made fully black for seamless integration into a product or environment. After scale-up, Lightricity's technology (albeit more expensive at present) is expected to achieve cost parity (per μW) with Silicon for small size devices (mm^2-cm^2).
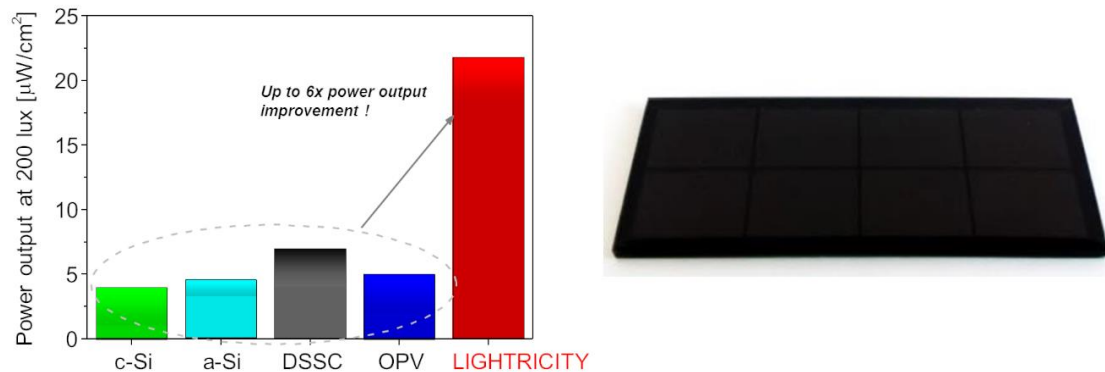
Figure 11 Comparison of indoor Photovoltaic (PV) Energy Harvesting technologies (left)
Current Lightricity macro-scale (2cm x 5cm) PV Energy Harvesting prototype module (right)

In addition to PV energy harvesting technologies, there are other methods of harvesting that could compete with PV harvesting, especially in industrial applications. These rely on either thermal gradient [61] (Thermoelectric Generators/European Thermodynamics), vibrations [62] (electrodynamic, piezoelectric) or electromagnetic [63] (wireless RF energy/Freevolt).
However, thermoelectric generators require a heatsink and are too bulky to be used in a card-like design such as the one we aim to develop in this project.
RF chargers and piezo-electric generators have typically smaller sizes that are suitable for integration but have power densities at least one order of magnitude less than Lightricity PV energy harvester (>20μW/cm^2 at 200 lux) when they rely on a standard environment, or rely on an external high power source such as a high magnetic flux, or a mechanical excitation to deliver usable power. Therefore, we believe that they will not be suitable for the applications targeted in the AMANDA project.

2.6.2   Batteries

IoT devices offer battery challenges that are different from other electronic devices. The batteries need to have a small footprint and thickness, be able to be trickle charged, charge only when the energy harvester can get energy, support wide temperature ranges and have long life span.
Miniaturizing incumbent solutions such as coin cells or cylindrical cell is a first option:
- Coin-cells: Miniature rechargeable coin cells from giants Panasonic and Varta exist which offer the same energy density advantage as larger coin cells. However, because coin cells require a rigid metallic casing, there is a limit to how small these batteries can be as shown in the Figures below:

Figure 12 Panasonic miniature coin cells (ML series)

ML COIN CELLS

| Model Number | Electrical Characteristics 20°C (68°F) | | Recommended Drain | Dimensions (Max.) | | |
	Nominal Voltage (V)	*Nominal Capacity (mAh)	Standard (mA)	Diameter inch (mm)	Height inch (mm)	Weight oz. (g)
ML414[1]	3.0	1.2	0.005	0.19(4.8)	0.06(1.4)	0.003(0.09)
ML421	3.0	2.3	0.005	0.19(4.8)	0.08(2.1)	0.004(0.11)
ML614[1]	3.0	3.4	0.01	0.27(6.8)	0.06(1.4)	0.006(0.16)
ML621[1]	3.0	5.0	0.01	0.27(6.8)	0.08(2.1)	0.008(0.23)
ML920	3.0	11.0	0.03	0.37(9.5)	0.08(2.0)	0.014(0.4)
ML1220	3.0	17.0	0.03	0.49(12.5)	0.08(2.0)	0.03(0.8)
ML2020	3.0	45.0	0.12	0.79(20.0)	0.08(2.0)	0.078(2.2)

* Nominal capacity shown is based on standard drain and cut off voltage down to 2.0V at 20°C (68°F)

[1] Available as a bare cell.

Figure 13 Panasonic ML series coin cells

Figure 14 Varta small size coin cells

Type Designation	Voltage (V)	Capacity (mAh)	Diameter (mm)	Height (mm)	Length (mm)	Width (mm)	Weight (g)
CP 1254	3.7	50	12.1	5.4			1.6
CP 1654	3.7	100	16.1	5.4			3.2

further sizes in development

Figure 15 Varta CP series coin cells

The Swiss company Wyon Technologies is using a stacking rather than a rolling method to pack their coin cells, which allow them to yield 160µAh for a 2mm diameter, 2mm height coin cell

Figure 16 Wyon Technologies miniature coin cells

MICRO TECHNOLOGY

Apart from chocolate and cheese, Switzerland is also known for competences in micromechanics. Wyon has well-grounded expertise and longstanding experience in this specialist area and can produce rechargeable Li-Ion batteries in micro sizes thanks to this knowledge. The following micro battery was developed for an implant and is intended for a life span of 10 years.

Product specifications:

|	
Chemical System	LCO/Graphite
Voltage Range	4.2 — 3.0 V
Rated dis. capacity @ 0.5 Rate	160 µAh
Nominal Voltage	3.7 V
Cell design	stacked electrodes
Weight	0.016 g
Case material	Titanium
Size	Ø 2 mm, height 2 mm

2 mm

© wyon swiss batteries

Figure 17 Wyon Technologies miniature coin cells specs

Miniature cylindrical cells have been developed mainly for the benefit of medical implants by companies such as GreatBatch (now Integer), Quallion and Eagle Picher: these have good life cycle (500-1000 cycles) and an energy density similar to larger size cylindrical batteries.

10.9 mm

2.6 mm

1.5 mAh

20.5 mm

7.5 mm

3 mAh

35 mm

17 mm

200 mAh

Figure 18 Quallion miniature batteries

In summary, miniaturising incumbent solution keeps the long life, high energy density aspects of larger size batteries up to a point only, when casing becomes a relatively high proportion of the battery and energy density is reduced significantly.

Solid-state batteries tackle these challenges, by providing both a flat aspect ratio with thickness <1mm and good energy density. Solid-state batteries use solid electrodes and solid electrolytes instead of the polymer or liquid ones that lithium-polymer or lithium-ion batteries use. They have high temperature tolerance and are considered safer, since they do not use liquid electrolytes who are flammable. They can also be manufactured in very flat form factor well below 1mm, application for insertion in a smart sensing card. Several solid-state battery manufacturers have existed and retired over the last decade, possibly because the IoT market was not large enough, or because all these manufacturers were essentially making various version of the same battery: companies like IPS, Cymbet, Front Edge technology and ST Microelectronics licensed a technology developed by Oak Ridge National Labs in the 80's and developed their products using the same process but with different shapes and sizes. Unfortunately, this process which uses a high temperature processing step, was eventually shown to degrade the battery specs and lead to short cycle life.

Commercialising solid-state batteries for IoT applications has been difficult: ST decided to stop this side of their business in 2018; IPS was acquired by Apple in 2012 but no product was ever commercialized by Apple and it is likely that the project was dropped; Cymbet invested in large volume production equipment and in 2016, but could not get enough orders to maintain this level of equipment and they are now only selling real time clocks; Front edge Technology have a small pilot line and only concentrate in small volume orders.

Ilika's Stereax® solid-state batteries are produced using a low temperature route which avoids the failure mechanism described above: the have several benefits over currently available lithium-ion batteries. Their life span is up to 10 years, they are faster to charge, have low leakage currents, are not flammable, can be integrated into ICs and have a small footprint.

Manufacturer	Ilika [64] Stereax® M250	Cymbet [65] CBC050	FET (no product name)	ST Micro EFL700A39
Dimensions	12mm x 12mm	5.7mm x 6.1mm	25.4mm x 25.4mm	25.4mm x 25.4mm
Thickness	< 750µm	0.2mm	0.15mm	0.22mm
Output Voltage (nominal)	3.5V	3.8V	3.6V	3.9V
Capacity (nominal)	250µAh	50µAh	1mAh	0.7mAh
Peak Current	5mA	100µA	-	10mA
Life cycle (1C)	900 (100% DoD)	1000 (50% DoD)	5000 (10% DoD)	4000 (75% DoD)
Nominal current	250µA	50µA	1mA	0.7mA
Temperature range	-20 to 100°C	-40 to 75°C	To 160°C	-20 to 60°C
Internal resistance	120 Ohm	7000 Ohm	-	100 Ohm

Table 11 Solid-state batteries comparison

2.6.2.1 Academic research into Lithium batteries advances

Solid-state batteries are types of solid-state ionic devices discovered by Michael Faraday in the 1830's, with his work on silver sulfide and lead(II) fluoride [66]. They are also a type of lithium ion batteries, which were invented by John Goodenough, Stanley Whittingham, Rachid Yazami and Akira Yoshino during the 1970s–1980s [67]. The most common type of solid-state batteries, namely thin film batteries deposited by sputtering and using $LiCoO_2$ cathode, LiPON electrolyte and Li anode, was invented at Oak Ridge National Lab in the 1990s [68] as well as use of buffer layers to reduce interfacial resistance. Since this discovery, researchers have been trying to use different materials, vary processing techniques or manipulate the architecture of solid-state batteries to improve their performance and bring them to market.

2.6.2.1.1 Materials

Most of the research, in terms of materials, has been concentrated on discovering or developing a solid electrolyte with high ionic conductivity at room temperature with systems such as lithium superionic argyrodites Li_6PS_5X (X = Cl, Br, I) [69], lithium ionic conductor thio-LISICON: the $Li_2S - GeS_2 - P_2S_5$ [70] or $Li_4SiO_4 - Li_3PO_4$ solid electrolytes [71]. In 2013, researchers at University of Colorado Boulder announced the development of a solid-state lithium battery with a solid composite cathode, based upon an iron-sulphur chemistry that promised higher energy capacity [72]. In 2017, John Goodenough, the co-inventor of Li-ion batteries, unveiled a solid-state battery, using a glass electrolyte and an alkali-metal anode consisting of lithium, sodium or potassium [73]. A lot of research has been carried to use high-voltage cathode materials with solid-state electrolytes to increase the energy density [74]. Replacing Li by Na has also been a rich topic of research with the benefit of a lower production cost [75].
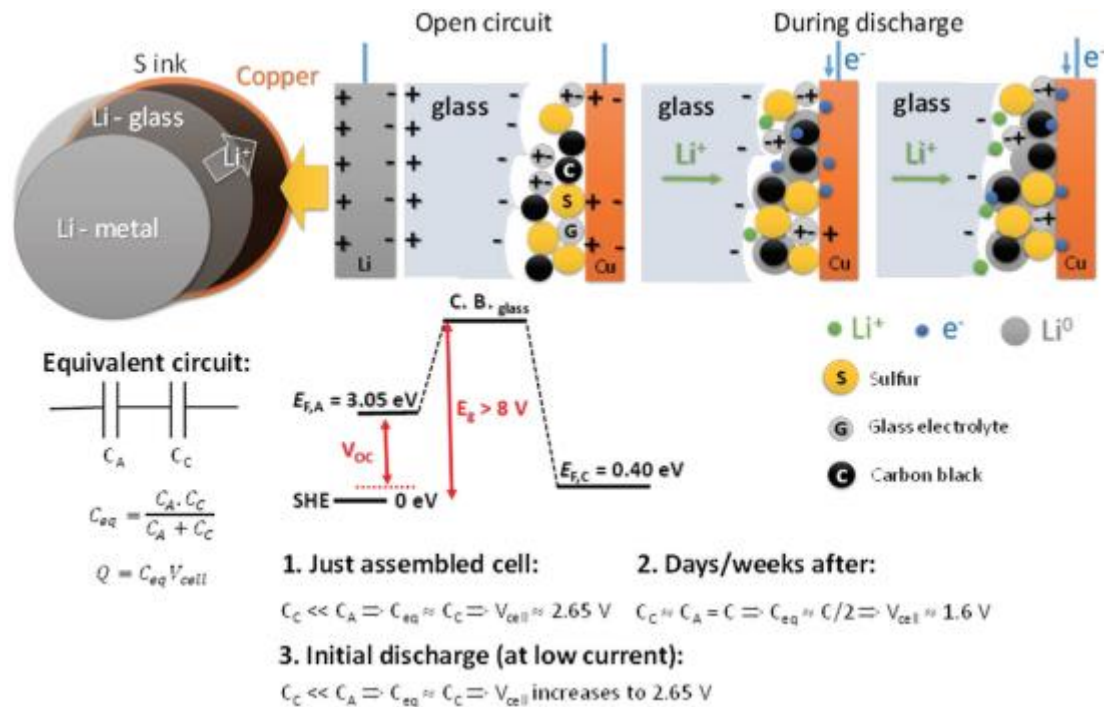
Figure 19 Charge / discharge process in glass solid-state battery developed by John Gooenough

2.6.2.1.2 Processes

In 2019, researchers at MIT developed a new pulsed laser deposition technique to make thinner lithium electrolytes using less heat, promising faster charging and potentially higher-voltage solid-state lithium ion batteries using a lithium garnet electrolyte component (chemical formula, $Li_{6.25}Al_{0.25}La_3Zr_2O_{12}$, or LLZO) with layers of lithium nitride (chemical formula Li_3N) [76], Figure 20. Yoshima *et al.* have investigated bipolar (or-two-sided) batteries in order to increase energy density [77]. Hayashi *et al.*, explored the mechanical milling of solid electrolytes [78].
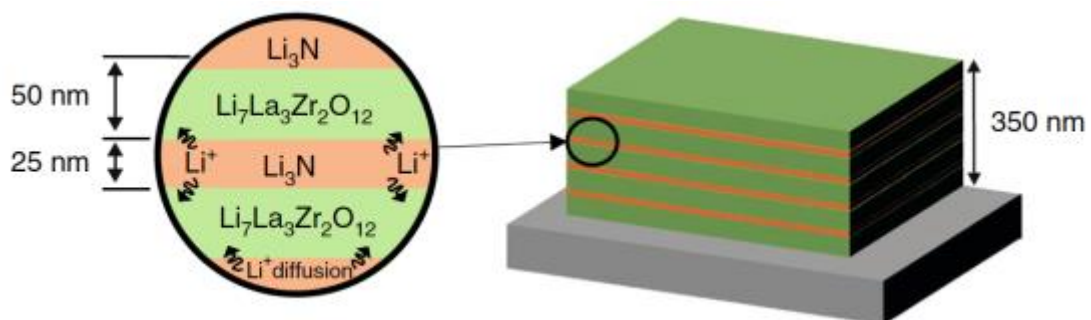
Figure 20 Graphic representation of solid-state electrolyte devised by MIT

2.6.2.1.3 Architecture

The main approach for increasing energy and power density in thin-film solid-state batteries has been to move from a planar, 2D architecture like that used in the Ilika Stereax batteries to be used in the AMANDA ASSC, to 3D frameworks, as reviewed in this paper by Oudenhoven *et al.* [79] and by Finterbusch *et al.* [80]. Atomic Layer Deposition has been successfully used to create nanometre-scale paths in solid-state cells [81], Figure 21.
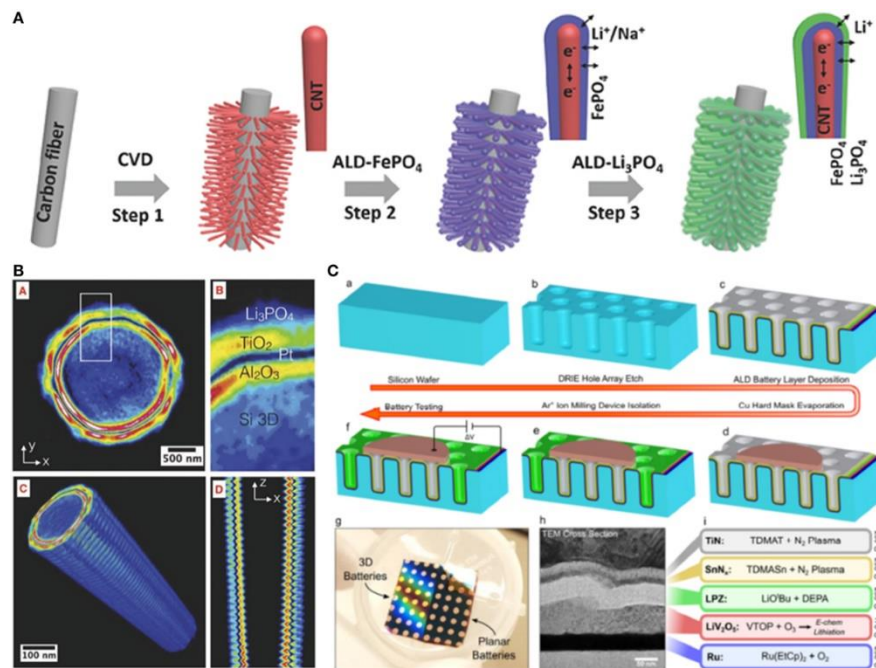
Figure 21 Process for fabricating 3D solid-state batteries

All of these developments are potentially significant, however in the timescales of the AMANDA project it is not expected that any can be integrated into the energy storage component.

2.6.3   Power Management
2.6.3.1   General purpose power management circuits
The market for power management integrated circuits (PMICs) dedicated to an operation with energy harvesters has a small number of players. It is explained by the fact that energy harvesting is a complex problem that has to face several challenges:

- PMICs must be adapted to the nature of the energy harvested (thermal, RF, solar, vibrational) leading each to different constraints such as very small input voltages for thermal energy, quick drop of the energy harvested if the operating point is set beyond the optimal voltage for solar cells, complex matching design to handle the high frequency of RF harvesting, etc.
- PMICs must be able to handle a variety of storage devices, from mF range capacitors to lithium-Ion battery. Each of these devices has different behaviour. For instance, capacitors or super-capacitors start with zero voltage which is not convenient for the start-up of the PMIC, dual-cell super-capacitor with 2 super-capacitors connected in series must be handled with a mid-point equilibrium circuit for a safe operation, batteries must be protected versus over-voltage or over discharge and while they are able to store a large amount of energy, they are not able to deliver a large instantaneous power due to their ESR.
- PMICs must handle power flows with several orders of magnitude fluctuations. This comes from the unpredictable nature environmental energy at the input, but also from duty cycled behaviour of the application circuits.

All these challenges make it very difficult to design an efficient PMIC for all different scenarios. Moreover, as the energy harvesting market is still emerging, there is not a system configuration used in most of systems helping the IC provider to avoid difficult trade-offs. Therefore, the energy harvesting PMIC market is dominated today by a portfolio of general-purpose products that although are able to work in many applications, they are optimum in none of these. As an example, most of the available PMICs have a cold start voltage between 300mV

and 600mV [82] [83] [84] [85] [86] [87] [88] [89]. Such a voltage allows to cold start the circuit without using an external transformer. However, this voltage is often insufficient to work with a thermoelectric generator with a low temperature difference between cold and hot plates. In response to this problematic, Linear technologies or Electronic Marin developed specialized ICs such as the LTC3108 [90] or the EM8900 extra module [91] which makes it possible to start from a few tenths of a mV. This performance is obtained at the price of significant drops in power efficiency as the input voltage increases, a limited input voltage range and additional bulky components.

Manufacturer	V_{min} cold-start	Input voltage operation
EPEAS AEM10941 [82]	380mV	0.05-5V
T.I. bq25570 [83]	600mV	0.1-5.1V
T.I. bq25505 [84]	600mV	0.1-5.1V
Analog ADP5091 [85]	380mV	0.08-3.3V
Analog ADP5090 [86]	380mV	0.08-3.3V
ST SPV1050 [87]	550mV	$0.150V$-V_{batt}
Linear LTC3105 [88]	250mV	0.225-5V
Cypress CY39C831 [89]	350mV	0.3 - 4.75V
Linear LTC 3108 [90]	20mV	$20 - 500$mV
EM EM8900 [91]	5mV	$5 - 200$mV

Table 12 PMIC V_{min} cold-start and input voltage operation

2.6.3.2 Low-power design

PMICs are at the heart of an embedded system, managing all the power flow. However, they do not contribute to the functionality of the system and therefore users wish they do not impact the power budget. For this reason, there is a struggle between providers to achieve the lowest quiescent consumption. This quiescent current is below 1μA for the EPEAS, Texas Instrument and Analog Devices references [82] [83] [84] [85] [86]. Some manufacturers are way beyond on this race such as Linear or Cypress with quiescent currents higher than 10μA [88] [89]. These references are therefore not suited for miniaturized systems found in wearable applications and where the volume available for the energy harvester is sometimes smaller than one cubic centimetre. Indeed, all the harvested power would be used to supply the PMIC itself.

This low quiescent current is only relevant if the PMIC is also able to handle very low input power from the harvester with a good efficiency. Therefore, special design techniques are used such as a discontinuous operation mode for the switching converters.

PMICs must also be able to cold start, meaning that the system must be able to start from the energy available from the energy harvester without using the storage device. This is mandatory for applications using a capacitor as the storage device because this capacitor is empty on the first start-up. Furthermore, it is often required that the PMIC will be able to restart on itself if the harvester has not provided energy for a long period of time and the system has run out of energy. This might be the case, for instance, after public holidays on a smart building where office lights have been turned off for weeks. During the system cold-start, most of the circuit peripherals are not available and the switching converters operate in a degenerated mode. The minimum input power required to cold start put therefore also a constraint on the minimum amount of energy that must be harvested by the system.

Manufacturer	Input power @ V_{min}	Quiescent current
EPEAS AEM10941 [82]	3μW	400nA

T.I. bq25570 [83]	15µW	488nA @2.1V
T.I. bq25505 [84]	15µW	325nA @2.1V
Analog ADP5091 [85]	6µW	510nA
Analog ADP5090 [86]	16.5µW	320nA
ST SPV1050 [87]	17µW	2.6µA
Linear LTC3105 [88]	-	24µA
Cypress CY39C831 [89]	-	32µA
Linear LTC 3108 [90]	-	6µA

Table 13 PMIC input power and quiescent current

2.6.3.3 Heart of the system

One key difference between existing references, are the available built-in functions and the number of external components, and therefore the system footprint, required to make them work. This last figure can become critical in portable system and particularly when the use of bulky components is required as in [90].

The following is a list of available functionalities:

- Output voltages to supply system loads. Some PMICs are only dedicated to the storage device management such as the bq25505 [84] while other deliver up to two clean supplies from LDOs such as the AEM10941 [82] or the ADP5090 [86]. PMICs without clean output voltages requires the use of additional DC/DC converters to supply the sensors, the radio transmitter and the MCU. The constraint of an external DC/DC converter imply an additional quiescent current to be considered and the need for additional external components.

- The use of energy harvesters requires to evaluate the best way to extract charges out of it. Some PMICs simply try to maintain the voltage at the harvester at a predetermined value [90]. However, most of the references perform a basic maximum-power-point tracking by evaluating periodically the open circuit voltage (VOC) of the harvester and by regulating the voltage across the harvester at a fraction of this VOC. The fraction is fixed thanks to external resistors [82] [83] [84] [85] [86] [87] [88] or at a preset value [82] [83] [84] [89].

- The use of a primary battery allows to ensure that the system will not run out of energy even when the harvester does not provide energy for a long period of time. In such a case, the system maintenance for battery replacement is lowered thanks to the energy harvested as the primary battery is only used sporadically.

Manufacturer	MPPT	Primary battery	Outputs	External components
EPEAS AEM10941 [82]	on-chip or external	yes	2 LDOs	7
T.I. bq25570 [83]	on-chip or external	no	buck	14
T.I. bq25505 [84]	on-chip or external	yes	-	10
Analog ADP5091 [85]	external	yes	2 switched reg. Output	16
Analog ADP5090 [86]	external	yes	2 LDOs	12
ST SPV1050 [87]	external	no	1 LDO, 1 switch	10
Linear LTC3105 [88]	external	no	-	17

| Cypress CY39C831 [89] | on-chip | no | - | 13 |
| Linear LTC 3108 [90] | No MPPT | yes | 1 LDO | 7 |

Table 14 PMIC MPPT, battery, outputs and external components

2.7 Wireless Communication

2.7.1 Low-Power Wide-Area Network Technologies

Low-power wide-area network, LPWAN, is a leading wireless communication technology for IoT networks. It enables a low power consumption, long range and lower bandwidth with lower bit rates [92] compared to other wireless wide area network technologies, such as GSM. There are a number of competing standards in the market that support the LPWAN technology, including both licensed and license-free platforms [93]. For example, LoRa and Sigfox are license-free, while NB-IoT and LTE-M need to be licensed.

2.7.1.1 LoRa

Long Range, LoRa, is a proprietary chirp spread spectrum radio modulation technology, integrated with forward error correcting capability [93] and it is patented by Semtech. A LoRa-based communication protocol called LoRaWAN was standardized by LoRa-Alliance [94].

Using LoRaWAN, each message transmitted by an end-device is received by all base stations in range. By exploiting this redundant reception, LoRaWAN improves the communication reliability ratio [94]. However, this adds to the installation cost, since additional base stations must be deployed. The resulting duplicate receptions are filtered out in the backend system and are also exploited for localization of the transmitting end-device [95].

The end-devices operate in three device classes to satisfy different requirements and different applications [92]. Class A devices accept bi-directional communication where each end-device's uplink transmission is followed by two short windows for receiving downlink messages [94]. These devices consume the least amount of power. Class B devices accept bi-directional communication, but with additional receive windows at scheduled times. Class C devices accept bi-directional communication with almost continuously open receive windows, resulting in a high-energy consumption.

2.7.1.2 Sigfox

Sigfox is an M2M communication technology that uses unlicensed frequency bands for radio communication [96]. It has been developed by the Sigfox company, founded in 2009 in France and is now operating in more than 30 countries. Sigfox Network Operators deploy proprietary base stations equipped with cognitive software-defined radios and connect to the backend servers using an IP-based network [95]. The end-devices connect to these base stations using Binary Phase Shift Keying modulation in an ultra-narrow band of 100 Hz, at a maximum data rate of 100 bps [94]. That way, Sigfox uses bandwidth efficiently and has very low noise levels, thus resulting in a low power consumption, low cost antenna design and higher receiver density.

The number of messages over the uplink is limited to 140 per day with a length of 12 bytes each, to conform to the regional regulations on use of license-free spectrum. The downlink communication occurs only after an uplink transmission has taken place. The downlink messages are limited to 4 with a length of 8 bytes. The reliability of the uplink messages is improved by the transmission duplication, as well as the use of time and frequency diversity. Each end-device can transmit the same message multiple times over different frequency channels. The frequency is chosen randomly by the end-devices, since the base stations can scan all the channels to decode the message, resulting in cost and complexity reduction for the end-device.

2.7.1.3 NB-IoT

NB-IoT is a narrow band technology, which aims at enabling deployment flexibility, long battery life, low device cost and complexity & signal coverage extension [95]. There are three possible deployment methods:

- Stand-alone operation, where it can be deployed inside a single GSM carrier of 200kHz
- Guard band operation, where it can be deployed using the unused resource blocks in an LTE carrier's guard-band
- In-band operation, where it can be deployed inside a single LTE physical resource block of 180kHz

NB-IoT uses single-carrier Frequency Division Multiple Access (FDMA) and Orthogonal FDMA in uplink and downlink, with a maximum throughput rate of 200 kbps and 20kbps respectively [94]. The payload size in each message can be up to 1600 bytes and a battery lifetime of 10 years can be achieved when transmitting 200 bytes per day on average. NB-IoT communication protocol is based on the LTE protocol, but reduces LTE functionalities to the minimum and enhances them for IoT applications [94] which results in reduced battery power consumption.

2.7.1.4 LTE-M

LTE-M allows for battery-operated IoT devices to connect directly to an LTE network without a gateway. LTE-M also supports the reuse of LTE technology. This means that legacy components do not require additional hardware and benefits from all the security and privacy of the mobile network features, such as entity authentication, confidentiality, data integrity and mobile equipment identification [93].

LTE-M operates on a 1.4MHz carrier or on six Physical Resource Blocks. The IoT device will always listen to the central six Physical Resource Blocks for control information. When an IoT transaction is due, it will obtain a number of consecutive PRBs within the spectrum of operation [97].

LTE-M introduces Half Duplex Frequency Division Duplex (HD-FDD) and its band support is limited to sub-GHz band for reduced cost. It offers 1Mbps downlink and 500bps uplink [93]. The IoT devices enter a deep sleep mode without the need to re-join the network upon wake up.

LPWAN technologies are suitable for multiple smart applications, but each technology has its advantages and disadvantages and can better satisfy the requirements of specific applications. The following Table makes a comparison of the LoRa, Sigfox, NB-IoT and LTE-M specifications.

Characteristic	LoRa	Sigfox	NB-IoT	LTE-M
Frequency Band	EU(433, 863-870MHz) US(433, 902-928MHz) China (470-510MHz, 779-787MHz) Asean (920-923.5 MHz)	EU (868MHz) US (902MHz)	Licensed cellular (LTE) frequency bands	Licensed cellular (LTE) frequency bands
Bandwidth	250KHz and 125KHz	100Hz	200KHz	1.4MHz
Coverage	Urban: 3–5km Rural: 10–15km	Urban: 3–10km Rural: 30–50km	15km	11km

Maximum Data Rate	LoRa: 0.3 - 37.5kbps FSK: 50 kbps	UL: 100bps DL: 600bps	UL: 250kbps DL: 170kbps	1Mbps
Maximum messages per day	Unlimited	UL: 140 DL: 4	Unlimited	Unlimited
Authentica-tion	AES - 128b	No	Yes	Yes

Table 15 Comparison of Sigfox, LoRa, NB-IoT and LTE-M Specifications [93]

In summary, IoT applications and use cases that require a higher bandwidth can use NB-IoT or LTE-M. Applications and use cases that do not transmit frequently, have small payload, a limited data rate and are battery-based, can use Sigfox or LoRa. For example, the smart farming, smart parking and environmental monitoring use cases are best fitted for Sigfox or LoRa, while applications like street light monitoring and control and industrial monitoring are best fitted for NB-IoT. Finally, asset trackers, patient monitors and smart watches are best fitted for LTE-M. The Table below provides a better understanding of the most preferable technology for each use case.

Sigfox, LoRa	**NB-IoT**	**LTE-M**
Smart farming	Street light monitoring and control	Asset trackers
Smart lighting	Industrial monitoring	Patient monitors
Smart parking	Gas/Smoke detectors	Smart watches
Smart temperature monitoring	Smart manufacturing	Fitness bands

Table 16 General IoT Applications and Technology Fittings.

There are still many issues and challenges regarding the IoT and LPWAN. Some aspects that are subject to future research include an interoperability between different technologies, security, scalability and overload.

2.7.2 Wireless Personal Network technologies

A WPAN is a personal area network carried over a wireless technology with a reach limited to a few meters. The most common technologies are Bluetooth Low Energy (BLE) and Zigbee. BLE (IEEE 802.15.1) is the IoT-oriented version of Bluetooth since it preserves its communication range by reducing the data rate down to 1Mbps and the power dissipated down by 20-100 times [96] compared to Bluetooth. BLE has been implemented in tablets and smartphones since 2012 with no need for other gateways or dongles [98]. Some advantages of this technology include a low cost, low latency, multi-vendor interoperability and easy application implementation for wireless devices [98].

2.7.2.1 Bluetooth Low Energy

BLE operates in the 2.4GHz frequency. It specifies 40 channels; 37 of those are used for bidirectional data communication and the other 3 for unidirectional advertising, while also using

a 128bit AES encryption. Some applications that use BLE are indoor localization, activity and proximity detection.

2.7.2.2 Zigbee

Zigbee (IEEE 802.15.4) is an IoT wireless communication technology used for monitoring, sensing and other low-power, low-bandwidth needs. It is designed for small-scale projects that require a wireless connection. Zigbee can carry small amounts of data over a short distance and has a very low power consumption. It supports star, mesh and mesh-tree network topologies. Moreover, it comes with security and interoperability application profile features [98]. Zigbee operates at a 2.4GHz frequency and has a predefined rate of 250KBps. Each Zigbee network consists of three different types of devices: Zigbee End-Device, Zigbee Router and ZigBee Coordinator. Additionally, Zigbee has a default 64bit message integrity, network layer authentication through a common shared network key and AES-128 encryption with a shared key that is distributed by a trustworthy device [96].

2.7.3 Discussion

In the AMANDA project there is a need for LPWAN features as well as for a WPAN communication system that could be used indoors or even between buildings that are not far from one another.

ZHAW has published scientific articles that deal with LoRa, Sigfox as well as Bluetooth Smart. These articles have been used to compile many of the conclusions of the rest of this Section [99] [100] [101].

For LPWAN communications, there are several elements that should be considered when comparing solutions.

Energy: How much energy the solution requires to deliver the average data payload?

Coverage: How many countries already have providers that support the system? What is the penetration in the country now and in the future?

Range: How far apart can devices be and still communicate?

Basically, the use of maximal transmitting power helps to achieve better range (+14dBm in case of LoRa/Sigfox in Europe, 868MHz band).

Frame size: How much data can be sent in a frame?

Reliability: How reliable the communication is? Licensed bands (NB-IoT) are basically more reliable than unlicensed bands (Sigfox, LoRa). The possibility to repeat can be helpful and is linked to bidirectional communications.

Bidirectional coms: How many frames can be sent in an upload and download direction?

Availability of transceivers and stack: How many transceiver manufacturers support the protocol?

Technology	Sigfox	LoRa / LoRaWAN	NB-IoT
Coverage	Good (available in many EU countries)	Best (also available in many countries. Possible to set an own network gives the edge)	Acceptable (still being introduced. First test now in CH possible. Will get better)
Reliability	Good (transmits 3 times on narrow bands)	Acceptable	Best (Licensed band)
Payload size	Very small (max 12 bytes)	Depends on the SF.	Good
Data rate	Really low. 100bps	Depends on SF. 300bps in SF12	Good
Max UL/DL	Very small. 144/4	Acceptable: 144/14 (e.g. Swisscom in CH)	Good
Range	Kms	Kms in SF11, SF12	Kms (lower Rx sensitivity than LoRa)
Energy	High (for the size of the frame)	Acceptable	Acceptable
Peak current	Good	Acceptable	Worst. Can be a serious issue for Amanda
Device choice	S2-LP (ST) [18] Transceiver only Transceiver that can be used for Sigfox Rx 8.6mA , Tx (+14dBm) 20mA VDD: 1.8-3.6V QFN24L (4x4mm)	SX1261/2 [19] (Semtech) transceiver only VDD: 1.8V – 3.7V Lowest sleep/Off: 160nA, Osc + retention: 1.2µA Tx:45 mA @+14dBm, Rx :8.2mA Package: QFN 24	nRF9160 [20] NB-IoT SIP. GPS/NB-IoT/LTE-M 64MHz Cortex-M33. 1MB flash, 256kB RAM Package: 10 × 16 x 1.2mm LGA Throughput (UL/DL) LTE-M: 300/375kbps NB-IoT: 30/60kbps Rx sensitivity: LTE-M: -108dBm

---

[18] S2-lp datasheet. https://www.st.com/resource/en/datasheet/s2-lp.pdf , https://www.st.com/en/embedded-software/stsw-s2lp-sfx-dk.html
[19] LoRa transceiver. https://www.semtech.com/uploads/documents/DS_SX1261-2_V1.1.pdf
[20] Nordic nRF9160 NB-IoT SIP. https://www.nordicsemi.com/-/media/Software-and-other-downloads/Product-Briefs/nRF9160-SiP-10.pdf?la=en&hash=17944CE06A8877860196F155993923992CD57522
nRF9160 datasheet. https://infocenter.nordicsemi.com/pdf/nRF9160_OPS_v0.7.1.pdf

		Rx sensitivity: BW_L = 125kHz, SF = 7 -124dBm BW_L = 125kHz, SF = 12 -137dBm	NB-IoT: -114dBm Support: eDRX, PSM VDD: 3.3 - 5.5V Active Tx current (+23dBm) > 250mA (peaks can reach 380mA)
Alternative solution	Several other manufacturers have transceivers for Sigfox: On Semi, TI and others	SX1272 Previous generation. Requires more energy	SARA-N2xx[21] module: bands 8, 20 (u-blox) Data rate: up to 27.2 kb/s DL, 62.5 kb/s UL 96 pin LGA: 16.0 x 26.0 x 2.4mm, < 3g VDD (2.75 -4.2). Rx sensitivity: -135dBm Deep-sleep: < 3µA Active mode: < 6mA Rx mode: < 46 mA, Tx mode: < 220mA -40dBm 74mA, -7dBm 75mA, 3dBm 78mA, 13dBm 100mA, 23dBm 220mA
Other solutions [22]	-	-	SARA-N3xx [23] module: bands (u-blox) VDD: 3.6V (2.7 -4.2) Data rate: up to 125kbit/s DL, 140kbit/s UL 96 pin LGA: 16.0 x 26.0 x 2.4mm, < 3g Deep-sleep: < 3µA other currents: na

Table 17 Sigfox, LoRa, NB-IoT comparison

---

[21] SARA-N2 Series datasheet : https://www.u-blox.com/sites/default/files/SARA-N2_DataSheet_%28UBX-15025564%29.pdf
[22] Other NB-IoT module: https://www.quectel.com/UploadFile/Product/Quectel_BC95_NB-IoT_Specification_V1.4.pdf
[23] SARA-N3 series product summary. https://www.u-blox.com/sites/default/files/SARA-N3_ProductSummary_%28UBX-18012985%29.pdf

2.7.3.1 LoRa

Unlicensed Sub GHz bands. Coverage: several countries in Europe. Users can also setup their own systems, gateways. This is an important feature.

Most transceivers come from Semtech. ST and Microchip seem to be working on SoCs. The best range is achieved for SF12 and +14dBm. According to ZHAW measurements, that will require at least 100mJ for acceptable frame size. Tens of bytes.

2.7.3.2 Sigfox

Unlicensed Sub GHz bands. Coverage: several countries in Europe. No own system. An operator is necessary.

Transceivers are available from several firms. Max payload size is 12bytes, which is too little for this application. Energy consumption is estimated by ZHAW to be higher than for LoRa, since the device needs to transmit 3 times. The return channel is judged to be insufficient (max 4 down links), allowing only very simple applications. That will be too restrictive for this project.

2.7.3.3 NB-IoT

Projected to be important and dominant. Licensed band and therefore more reliable than LoRa or Sigfox. But higher fees expected.

Energy requirements seems to be of the same order as LoRa. However, peak currents are very high. NB-IoT may require the use of SIM cards which will lead to serious issues with thickness in this project.

2.7.3.4 Bluetooth Smart

We have not found any commercial stand-alone transceiver for BT. It will also be necessary to have a BT stack, which is often available in SoC solutions. For that reason, it is best to stick with SoCs. Criterial for comparison are dealt with in the papers [100], [101] from ZHAW. The Table related to embedded CPUs also considers SoA BT SoCs.

2.7.3.5 ZigBee, Thread, 6LoWPAN

These are based on the 802.15.4 layers and allow the implementation of mesh networks. These networks are not as popular as Bluetooth Smart (in terms of quantities). Many manufacturers of Bluetooth Smart devices also have 802.15.4 transceivers integrated in their solutions. This is the case of the best solutions that we present for Bluetooth Smart.

2.7.3.6 Positioning / Location (indoors and outdoors)

GPS is normally used. However, it is poor to impossible when one is indoors. For this project it is therefore important to find ways for indoors and outdoors positioning/location.

The recent adoption of BT 5.1 opens a path for indoor locations using AoA for devices with BT. In the case of 802.15.4 bases standard, another solution should be found (such as using a dual 802.15.4/BLE transceiver).

For outdoors, the traditional GPS approach can be used if good accuracy is required.

A LoRa LPWAN transceiver will allow the use of positioning methods associated with LoRa, as long as appropriate gateways are available.

Solution	Advantages	Disadvantages	Discussion
EPEAS processor + WPAN transceiver + LoRa, Lora positioning	Lowest cost.	Which transceivers for Bluetooth? BT stack needed in EPEAS processor.	Solution unlikely. Little is known about EPEAS processor now. Is there a BT stack for that device? Is positioning adequate enough?
EPEAS processor (master) RSL10 as BT and co-processor. LoRa, LoRa positioning	Can SIP be used to simplify system design? (required thickness) Lowest embedded and BLE energy	802.15.4 protocols unsure Limit at 3.3V (instead of 3.6V)	Ok if 802.15.4 protocols not needed. Might need to clear support issues. Is positioning good enough?
EPEAS processor (master) nRF52811 as WPAN LoRa, LoRa positioning	5.1 positioning features available 802.15.4 supported BT Smart supported	Slightly more power than the RSL10	Is positioning good enough?
EPEAS processor (as master) nRF52811 as WPAN LoRa or Sigfox for Long range GPS for positioning	GPS gives better accuracy	More devices, more power, more space	-
Positioning possibilities			
The ZOE-M8B of ublox is a low power GPS device. 8mA for tracking at 1Hz and 1.8V https://www.u-blox.com/sites/default/files/ZOE-M8B_DataSheet_%28UBX-17035164%29.pdf			
GPS positioning	Precise outdoors (about 1 to 2m)	Extra chip, space Energy consumption high Nordic NB-IoT SIP integrates GPS	Issue of peak current and thickness if NB-IoT used
LoRa positioning	Low-cost No extra energy or space	20 to 200m positioning accuracy	Good enough for many cases?
AoA (e.g. using Quuppa system)	Works well. 10cm to 40cm accuracy	Mounting of support antenna and HW needed	Good option for indoors

Table 18 Possible combinations for embedded, wireless, positioning systems

2.8   Packaging

There are several Encapsulation Methods, both in development and in the market, right now. This Section provides an overview of these techniques, the main issues AMANDA wants to tackle and the essential qualities that need to be regarded by this project. Lastly, a detailed sensor by sensor encapsulation analysis is presented to illustrate the reasoning behind the choices that will occur concerning the packaging of the end product.

2.8.1   Energy harvester packaging

Energy harvesting packaging includes encapsulation and interconnection of PV cells, including access to electrical contacts for connection with the system electronics.

Typical encapsulation for flexible PV energy harvester (e.g. amorphous Si solar cell) involves a protective film (PET or equivalent) that is laminated on either side of the cell. Interconnection of cells in series is typically done monolithically. This type of packaging can only withstand a limited temperature range (<<100°C) before failure. It is not compatible with Surface Mount Technique that would require process temperature up to 260°C.
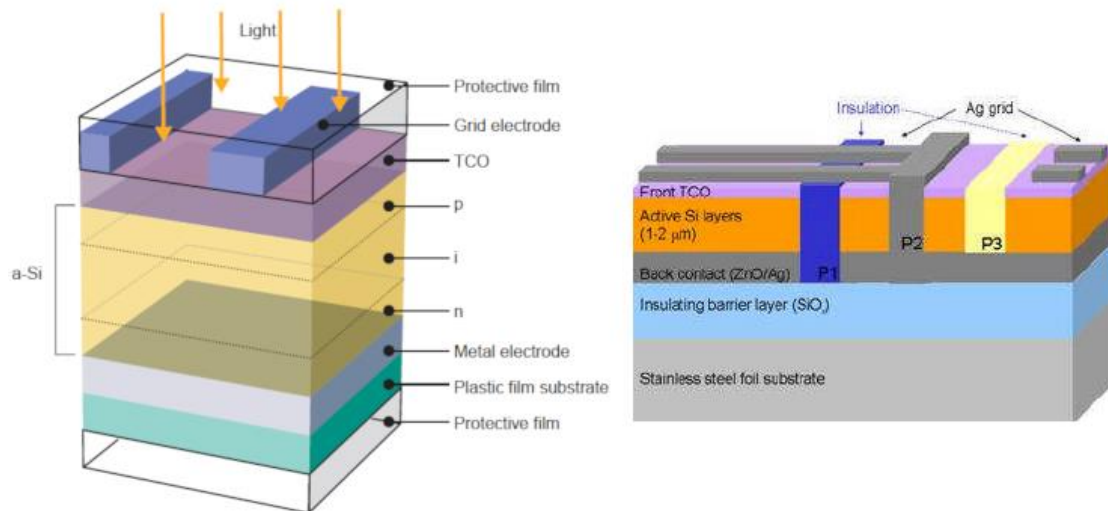

Figure 22 Amorphous Silicon structure including encapsulation (Panasonic) (left) Monolithic series interconnection (Panasonic) (right)

Figure 23 Access to electrical contacts (Amorphous Silicon energy harvester

Outdoor energy harvesters may include a glass cover and sealing for protection against moisture and water. The top protective layer may also be of Silicone or transparent epoxy, depending on solar cell type.

In this project, Lightricity will follow SoA semiconductor packaging process that uses PV die assembly onto a FR4-substrate, wire-bonding for interconnection, and rear pads for SMT attachment onto a host PCB. Compression/transfer molding (with Silicone encapsulant) and

dam-and-fill process (with transparent epoxy) are conventionally used for encapsulation [102].
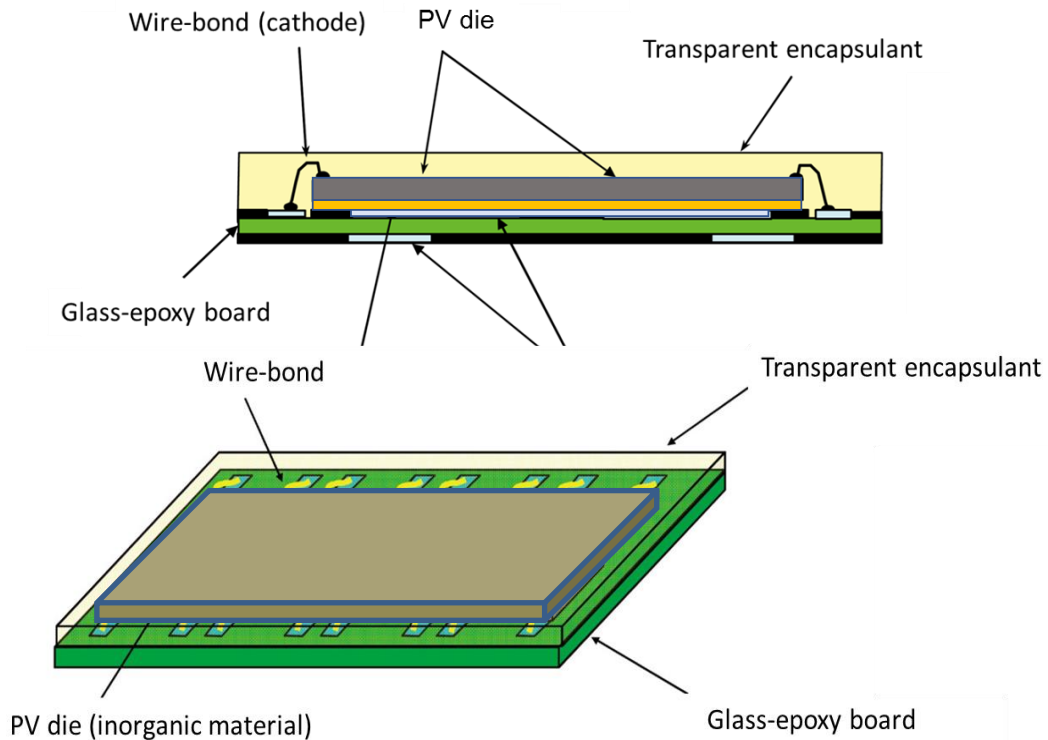
Figure 24 Cross-section of SoA semiconductor packaging method used for AMANDA (top) Top view of SoA semiconductor packaging method used for AMANDA (bottom)

2.9 PCB Design

Flexible electronics have emerged as a standalone field and matured over the past decades [103]. This type of PCBs offers the possibility to adjust the shape of devices making them an industrial standard for consumer electronics, wearables and medical implants, where thinness and the ability to curve are mandatory requirements for proper functionality. The development of organic and inorganic electronics benefited flexible devices and with the combination of either inkjet, screen or dispenser printing approaches [103] new devices have been developed, such as light-emitting diodes and organic solar cells.

As shown in Figure 25, one-side flexible PCBs contain several conductive layers, with a dielectric layer between them, on one side of the substrate. The conductive layers are interconnected by a via hole. One the other hand, double-side flexible PCBs consist of and an individual conductive layer on each side of the substrate, which are interconnected via a through hole as well [104]. Double-side flexible PCBs are usually manufactured by either inkjet or screen printing methods and they include a hole to electrically connect the two sides. A hybrid microelectronic system which combines both the printed functionalities and the silicon technology is used, most probably, to develop flexible electronic products like wearables [105]. When silver (Ag) material limitations are present, it is also necessary to use a copper (Cu) plating process in order to boost the electrical performance of a flexible PCB.
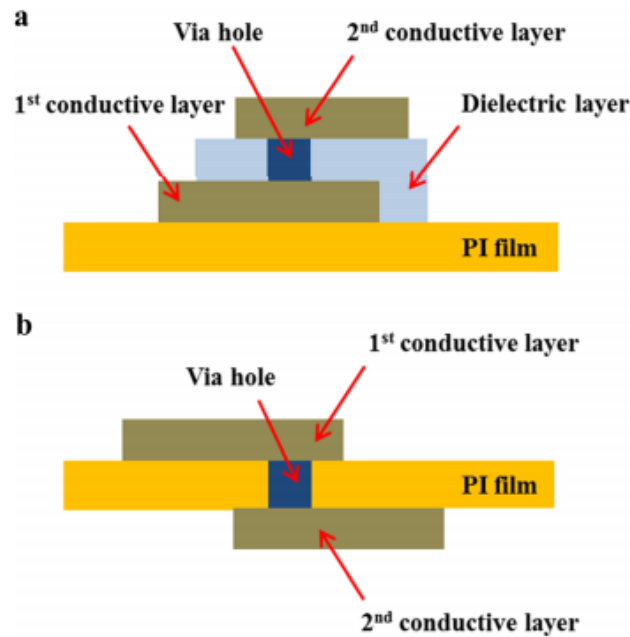
Figure 25 Design of double-sided FPCB attainable in printed electronics: a) two conductive layers with a dielectric layer in between on the one side of PI film and b) individual conductive layers on each side of the PI film with a through hole [104]

The advantages of flexible PCBs are that they can be bent and folded, generally taking advantage of all three dimensions. They reduce both the size and the weight of electronics, making them suitable for miniaturized and high-density devices. Their disadvantages include their susceptibility to damage, their high initial cost since they are developed for specific purposes and the difficulty to repair them or make changes, as their surface is covered with a protective film. Typical PCBs used today have a typical thickness of 1.55mm.
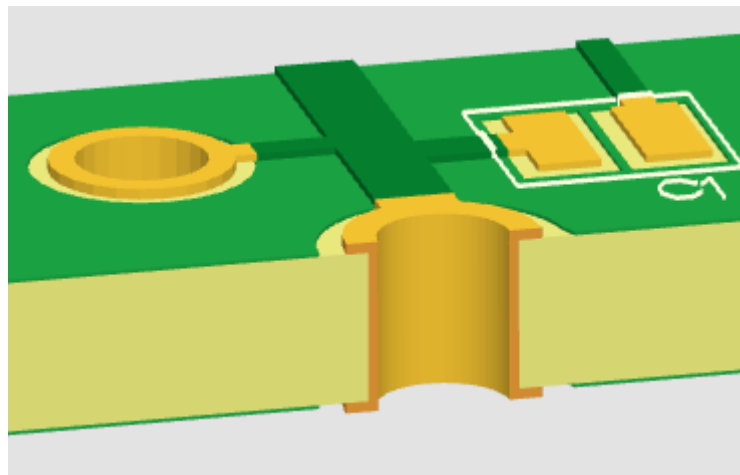

Figure 26 Typical 2 layer 1.55mm thick PCB

Thickness can go as low as 0.20mm and comes at an increased production cost compared to the typical thickness.
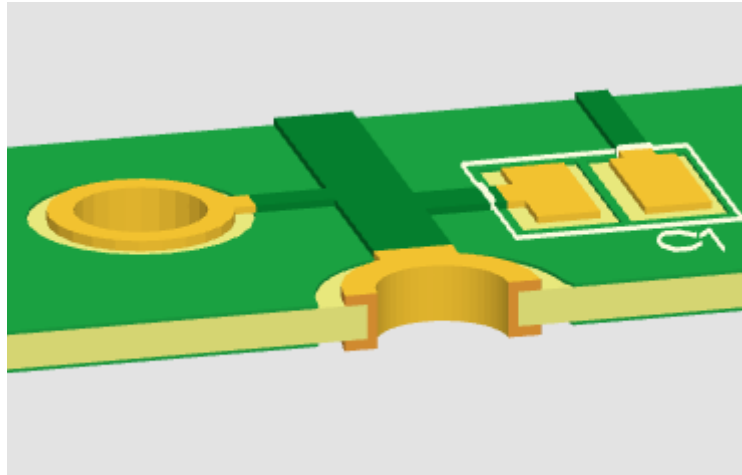
Figure 27 Double-layered 0.20mm thick PCB

Reducing PCBs' thickness has an impact on the number of copper layers a board can carry. For example, 0.20mm thick PCBs can only support two external layers. If two internal layers were required for a total of four layers, the minimum required thickness would be 0.36mm [106].
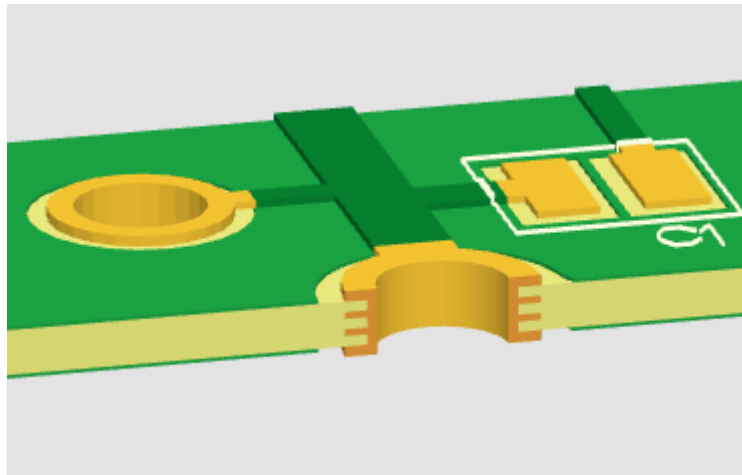

Figure 28 4-layered 0.36mm thick PCB

Another technology for circuit interconnection, instead of traditional PCBs, are flexible PCBs that can have a thickness as low as 0.12mm for a double-layered board.
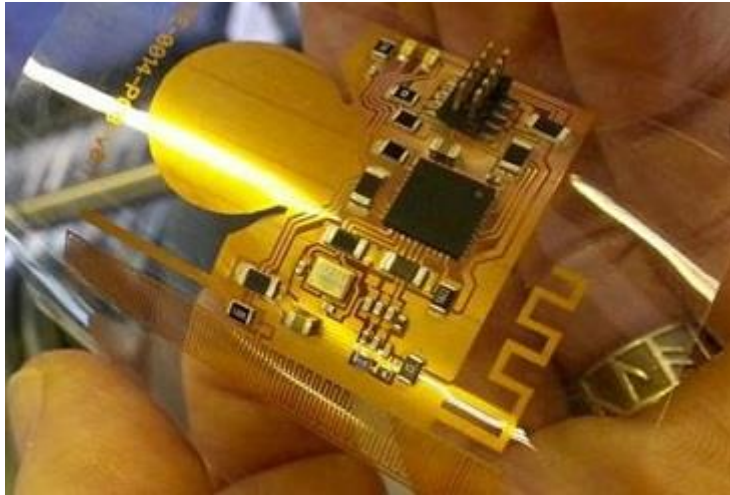
Figure 29 Single layer design on flexible material

A new technology that has recently hit the market involves 3D-printed circuit boards. The DragonFly™ Pro printer is offered by the Israeli company Nano Dimension. With the ability to print traces and spaces down to an accuracy of one micron, the DragonFly™ Pro inkjet deposition system is setting new accuracy and precision standards for 3D printed electronics. This allows the DragonFly™ Pro to deliver in industries with the most demanding design and quality requirements, such as aerospace, telecoms, healthcare and more.

The unique pairing of a dielectric ink optimized for mechanical support, thermal resistance and electrical insulation with a highly conductive nano-Silver ink that sinters at low temperatures is what brings PCB 3D-printing to life.
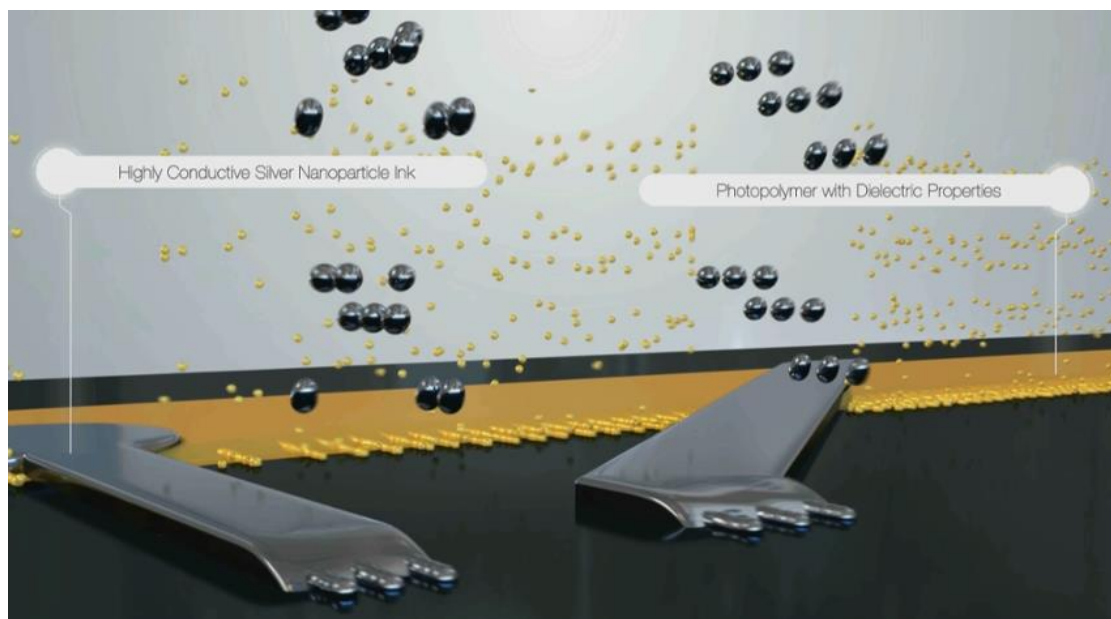
Figure 30 Highly conductive silver and dielectric polymer inks combined

The printer is able to combine these inks to print a full range of multi-layer PCB features, from intricate geometries to interconnections such as buried vias and plated through holes, seamlessly into multi-layer PCBs for agile product development. The result is a high quality, densely packed PCB, ready for component placement and soldering. Rigid-flexible designs and printed antennas can also be implemented.
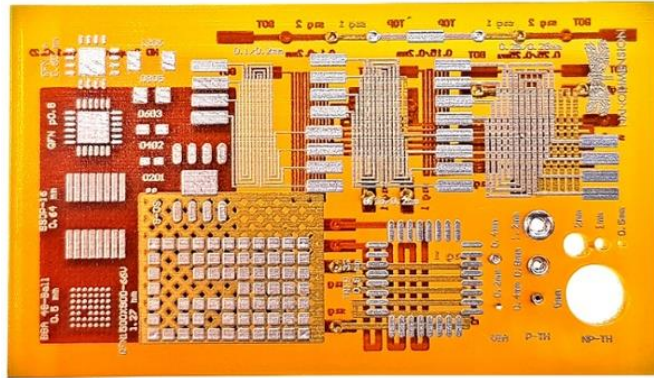
Figure 31 3D printed 4-layer design

Figure 32 Rigid-flexible design (left), antenna (right)

Modern electronics demand an improved performance, functionality and increased miniaturization. This creates the need for curved surfaces and 3D printed layers that are not flat or of uniform thickness. The challenge is to produce optimized electronic prototypes, embedding the electronics in any shape, in order to authenticate new product designs. This is where non-planar printing that this system is capable of can fit.
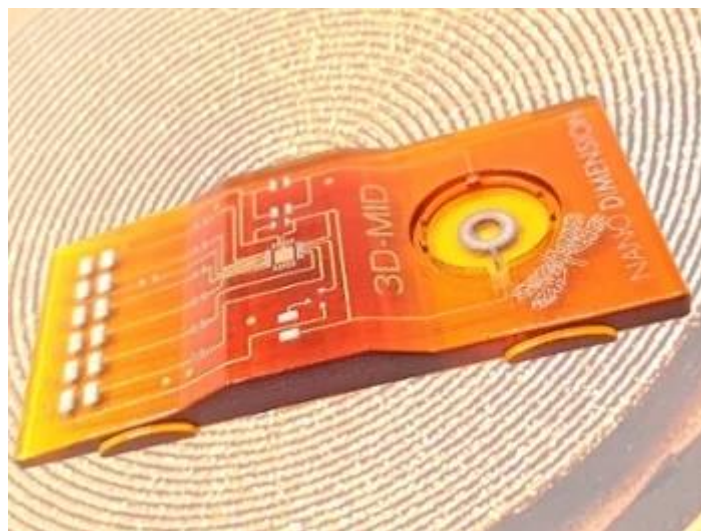
Figure 33 3D-printed non-planar design ready to host electronic parts

2.10 Miniaturization

Miniaturization is vital for applications where space is limited. Flexible PCBs help in the miniaturization, as described above. Stacking layers [107] also take advantage of the 3D space. They

use a stackable connector system or an MID technology which provides selective metallization in 3D on injection molded thermoplastic substrates and housings [108]. For the AMANDA project though, taking advantage of the 3D space is not an option, since the goal is to fabricate a credit card-like PCB. The electronic packaging can help to achieve further miniaturization, by using 3D interconnection schemes and stacking dies. Different technologies can be used depending on the application. These technologies can be defined as 3D-SIP, 3D-WLP and 3D-SIC [109].
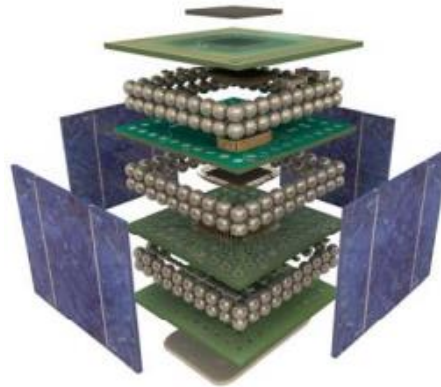
Figure 34 3D-SIP 1cm³ eCube by IMEC

2.10.1 Ultra-thin chip package

Ultra-thin chip package (UTCP) can be used to reduce PCB thickness since it is an enabler for die embedding in flexible PCBs [110].
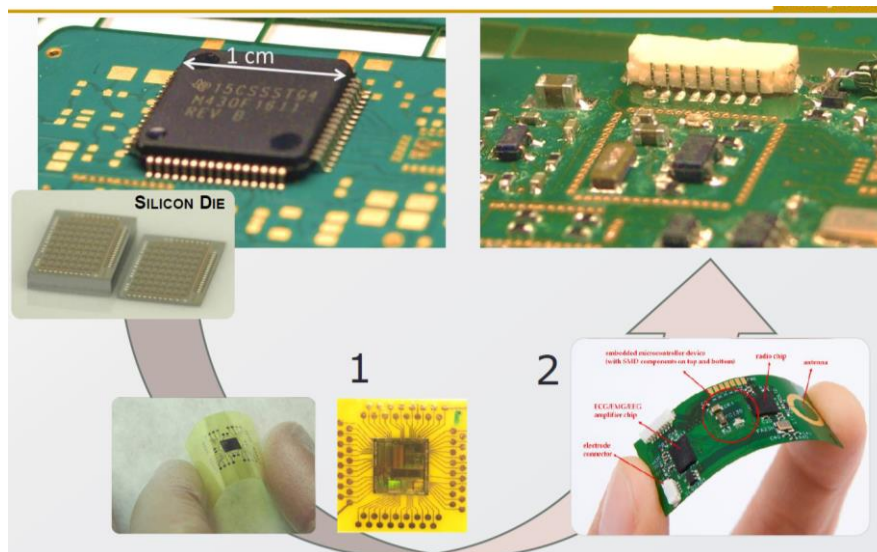
Figure 35 Flexible PCB with UTCP technology [110]

2.10.2 Printed electronics

Printed electronics is another way to reduce the PCB thickness. Printed electronics components, such as displays, antennas and transistors can be integrated into products as depicted in Figure 36.
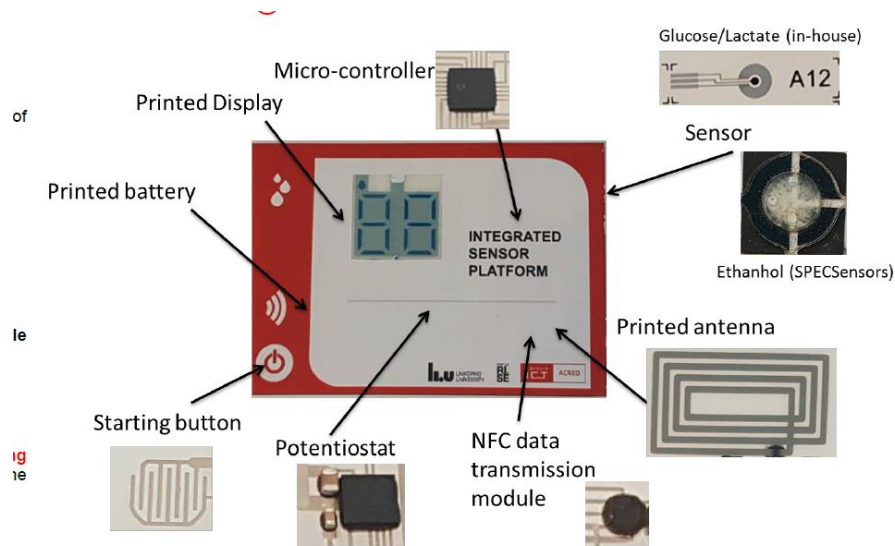
Figure 36 Device for real-time and remote monitoring of lactate [111]

2.10.3 Eco

Eco is a self-contained, ultra-wearable and expandable wireless sensor platform under 1cm³ [112]. It uses a flexible PCB expansion connector for its digital and analog input and output, battery charging and firmware programming. The sensor node consists of an MCU/Radio, a 3-axial acceleration sensor, which measures acceleration and temperature, a light sensor, a 3.3V regulator, a battery protection circuitry, a custom Li-Polymer battery and an expansion port with 16 pins for digital inputs and outputs. These IOs include an analog input, SPI, RS232, 3.3V output, voltage input for a regulator and battery charging. The eco platform has been implemented to interactive art performances and spontaneous motion monitoring of preterm infants.

The data aggregator collects data from all the Eco sensors and transmits them to a wireless access point connected to a host computer. The development/base-station board can serve as an EEPROM programmer, debugger and battery charger or as a base station for the Eco nodes.
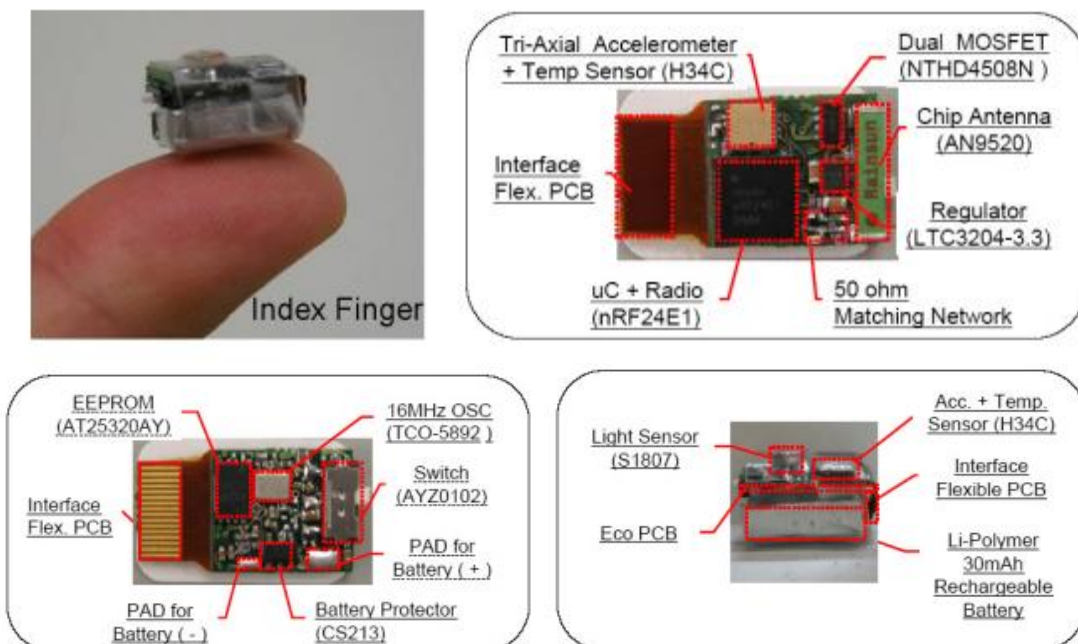
Figure 37 Eco sensor on a finger, top view, bottom view, side view [112]
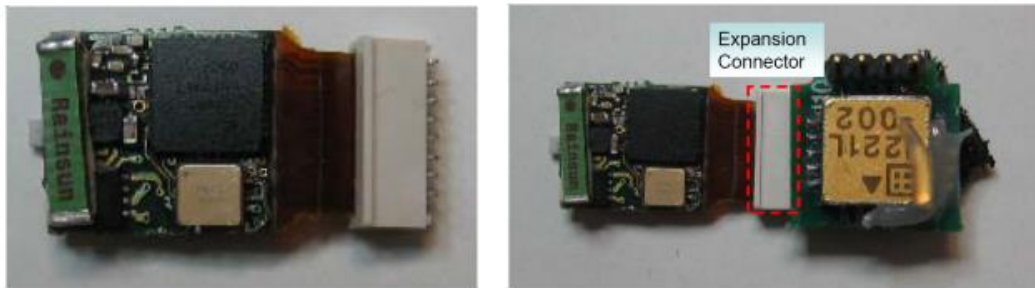
Figure 38 Expansion port with connector. Expansion sensor board [112]
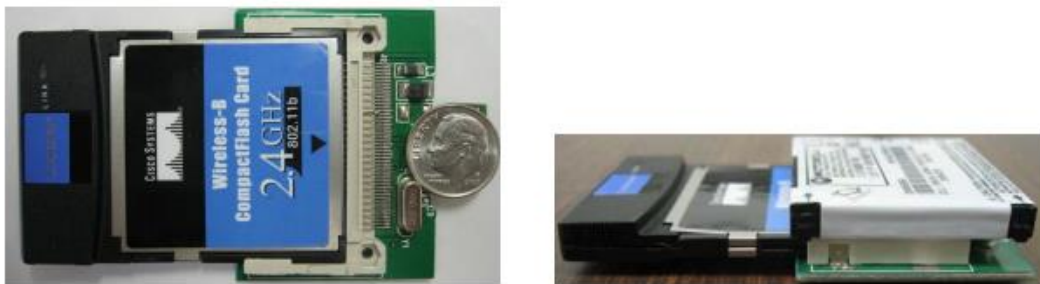
Figure 39 Data aggregator top and side view [112]
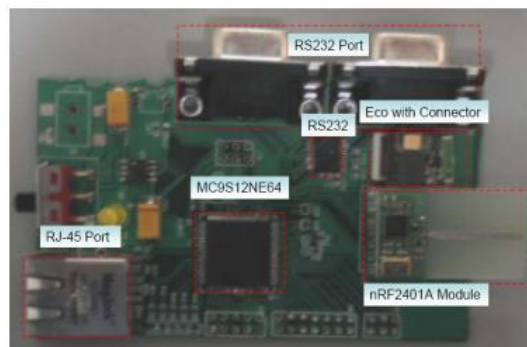
Figure 40 Development/Base-Station board [112]

2.10.4 bPart

bPart is a highly integrated autonomous sensor platform employed by mobile devices [113]. It consists of a BLE radio, an ambient illumination sensor, a 3D-acceleration sensor, a temperature and humidity sensor, a button and a magnetic switch for binary input. Moreover, it contains an RGB led for user feedback, a secondary led in the infrared spectrum which enables camera-assisted identification and tracking of the node and a lithium coin cell, all integrated in a volume of less than 1cm³. The bPart platform has been implemented on tangible interaction, indoor localization and physical web, activity tracking, participatory sensing and condition monitoring.

Figure 41 bPart sensor node next to an industrial grade sensor housing [113]

2.11 Wearables

The EKG shirt measures EKG signals. It consists of an EKG module on a flexible substrate, its encapsulation, a rechargeable flat battery, three EKG body contact electrodes and embroidered "wiring" and interconnections [114]. The module amplifies the signal between the right shoulder and the lower left rib using the left shoulder as a reference. Then, it processes the data and sends them via Bluetooth to a mobile phone or a PDA.

The size of the module is 27x27mm without counting the connector, which can be cut off after programming, with a thickness of 2.1mm. A 2.5mm thin battery is attached with snap fasteners for easy removal.

Figure 42 Shirt with electronics, snap fasteners for the battery and embroidered electrodes and conductor [114]

Both the conductors and the electrodes are embroidered with a conductive yarn.
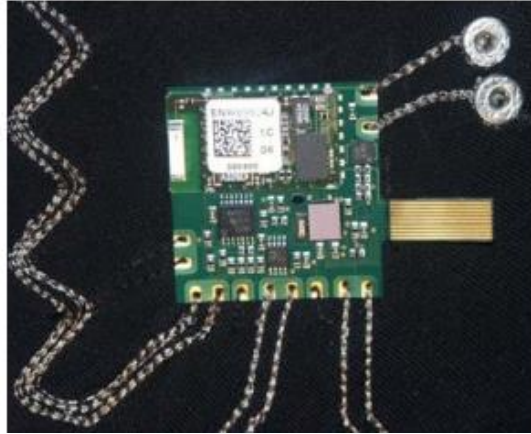
Figure 43 EKG module with a programming port, conductors to electrodes and snap fasteners for the battery [114]

The wearable sensor for electro-dermal activity [115] is able to record measurements to an on-board flash memory card, transmit them wirelessly and perform real-time analysis. The device consists of electrodes for the exosomatic EDA measurement, a triple-axis accelerometer, a digital signal controller, an analog to digital converter for sampling, a single Li-Polymer battery, a USB, a separate MCU in order to enable continuous measurements and a 2G micro SD card to store the data. If the data needs to be transmitted, a 2.4GHz transceiver module can be used. The architecture and the module are shown in Figure 44.
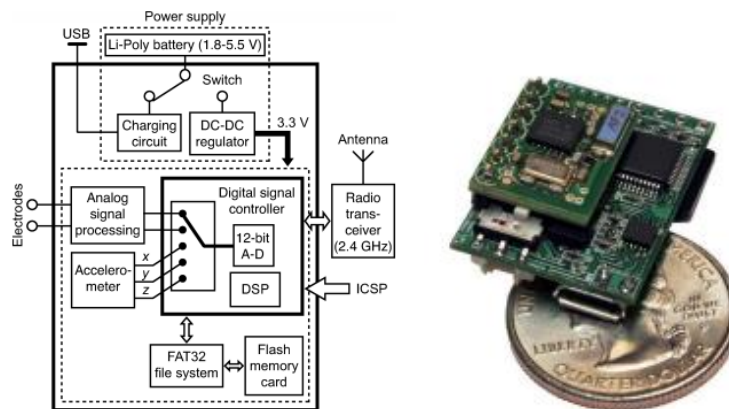
Figure 44 Architecture and EDA sensor module with radio transceiver on top [115]

The packaging makes the device inconspicuous making the EDA monitoring discrete, since the electronics are concealed in the wristband as shown in the following Figure.

Figure 45 Final wearable EDA sensor packaging [115]

A wearable FISA [116] is a flexible integrated sensing array designed for simultaneous and selective screening of a panel of biomarkers in sweat.
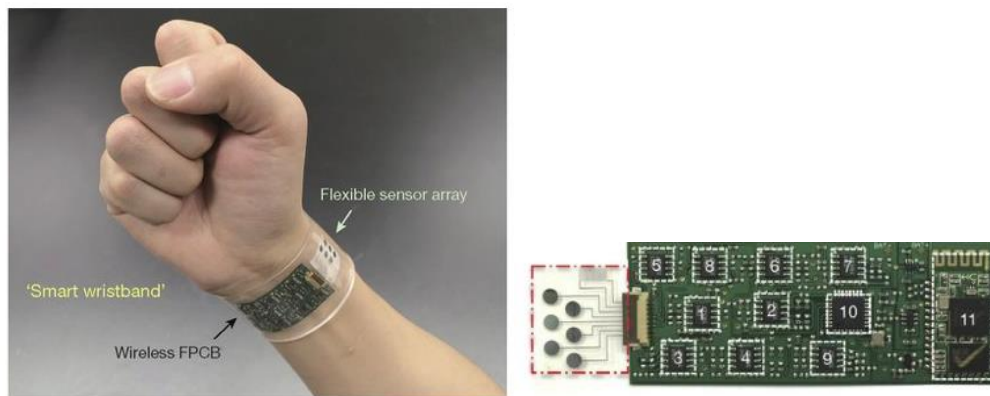
Figure 46 Wearable / Flattened FISA

It can be worn on various body parts, such as the wrists, the arms and the forehead. For the amperometric glucose and lactate sensors, a two-electrode system was designed. The FISA consists of Na^+ and K^+ selective sensors, lactate and glucose sensors, an ATmega328P micro-controller, a Bluetooth transceiver and a lithium-ion polymer battery. A custom mobile application was also designed to display the data.

2.12 Memory elements and other sensors

A list of serial memories in FRAM or ReRAM technologies that are especially appropriate for low power is presented below. Such elements can be used in order to save parameters or measurements (data loss prevention) when energy is low. Normally, they require less energy than flash memory and they have a much higher number of program/erase cycles.

Device / Characteristics	Packaging	Temperature range	Voltage	Frequency	Bandwidth
FRAM MB85RS64TU (2v0)	SOP-8, SON-8	-55 to +85°C	1.8 to 3.6V	10MHz (0.8mA)	64Kbit
ReRAM MB85AS4MT (1v0)	SOP-8, SPI	-40 to +85°C	1.65 - 3.6V	5MHz (0.2mA)	4Mbit

Table 19 Low power serial memory models

There are additional sensors that can be used in the AMANDA project. The following table lists magnetic sensors that can be used to detect the presence of magnetic fields.

Model	Output Type	Sensitivity	Range	Voltage Range	Sleep current	Measurement current	Principle	Remarks
LIS3MDL	I2C/SPI	6842 LSB/gauss	+/-2 to +/-16 gauss	1.9V - 3.6V	1µA	40µA – 270µA	magnetoresistive	x, y, z
TLE493D-W2B6	I2C	65uT/LSB	+/- 100 to 230 mT	2.8V - 3.5V	7nA	3.4mA	hall	x, y, z
MMC2460MT	I2C	1024 counts/gauss	+/- 6 gauss	1.62V - 3.6V	20nA	25µA – 60µA	magnetoresistive	x, y

Table 20 Magnetic sensors

Other sensors that are worth considering
The Bosch BME680 environmental sensor [117] is also worth considering. It has the following characteristics:

- 1.7 - 3.6V, 2.1µA at 1Hz humidity and temperature
- 3.1µA at 1Hz pressure and temperature
- 3.7µA at 1Hz humidity, pressure and temperature
- 0.09 - 12mA for p/h/T/gas depending on the operation mode

3   Guidelines

The AMANDA project should target a high user acceptability. It should be a clearly user driven project with user and technology provider interactions scheduled throughout its lifetime, having as an ultimate goal the realization of a functional system which can be potentially adapted to production. Moreover, demonstrated technologies should trigger commercial interest and allow for novel applications.

The project should deliver three versions of the system with divergent requirements. Due to the high level of miniaturization, only the core of the system should remain similar between all versions. Hardware/software of peripheral components should be dedicated towards requirements for that use-case.

The project is aiming for extreme miniaturization, meaning that, where it is possible, bare dies should be used.

The realization of AMANDA should adopt a start-up mentality; however, it should still include a good practice approach. In order to achieve success, the system flow listed in Figure 47 is proposed. It consists of many feedback loops where issues can be identified and removed. The flow consists of the following steps:

Clearly defined goal/goals

Based on project proposal and information from user functional description of the system should be written. The description should contain the functional features of the system with a clear indication of crucial and recommended properties.

Identifying the consortium technological strength

The partners of the consortium should provide information on the crucial parameters of their technical contribution to the project. Outstanding technology should be applied in the constructed system in order to achieve outstanding goals.

Translating needs towards a functional architecture with emphasis on the technological strengths of the partners and use cases

The system architects should analyse the goals and technological strength and propose concept/concepts of the system where the user demands will meet with technical capability. The architecture should provide technically possible ideas while fulfilling user needs.

Identifying consortium technological gaps and how they can be bridged

During the architecture development, gaps could be identified in the process flow (tasks that are not clearly allocated to any partner). Of course, the architecture should be developed such that these types of gaps are minimal, however sometimes they are unavoidable. It should be clearly identified where are the technological gaps and what is needed to fulfil them. The gaps should be presented to consortium and partners should agree who is the most suitable to take responsibility of such unassigned tasks [45].

Analysing the system and extracting parameters important for user

The architect should identify if the original request of the user can be fulfilled in 100%. If not, the architect should negotiate with the user about functionality and if necessary, to further adapt the architecture.

Documentation sharing

When the final system is approved by all stakeholders, the bill of material should be extracted and provided to relevant partners. At the same time, system information can be provided to the project's software developers. This way, hardware and software development can be performed simultaneously.

System production

In the production stage, assigned partners should gather required components and prepare techniques for manufacturing while partners responsible for software should prepare an initial version of the software.

System integration and testing

Hardware components should be integrated, and firmware should be installed. Functional testing should be performed. In case of doubts, there should be an interaction between integrators and hardware and software developers.

Enclosure production

The system should be packaged in a form that is usable in the proposed environment.

User tests and system realization

Technically functional system should be realized to user for stability test. In case of issues, the user should give feedback to the architect. Thus, the issue can be taken under consideration and possibly removed.
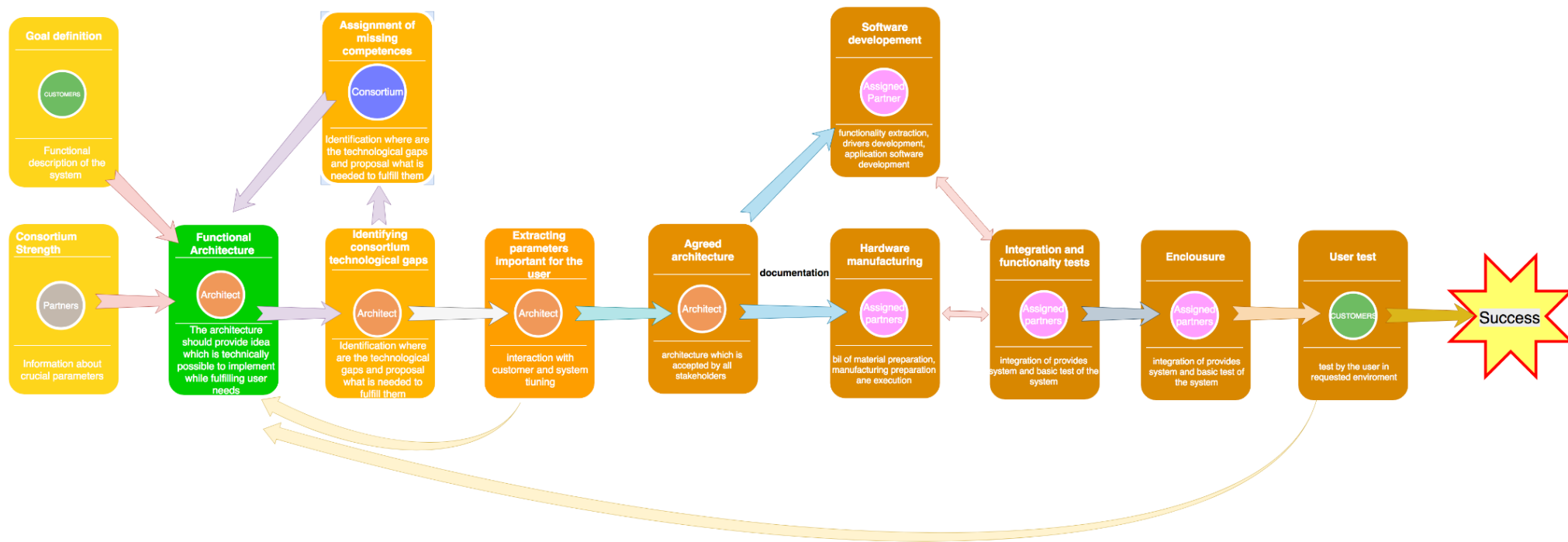
Figure 47 Proposed design and execution flow of the project

4   GAP Analysis

A preliminary SWOT analysis took place, in order to provide an overview of the consortium's actual performance and the basis to work upon. What became evident from the analysis is that most of the devices are and need to be more intelligent, interactive, trackable and able to connect to the internet of things. By 2020, around 1 trillion smart consumer products a year will be produced, leading to IoT smart platforms that will support them. Either existing or new enterprises need to be able to respond, launching new IoT platforms which will provide the customers with the ability to change the way they live and work. We can already see many companies approaching these innovative technologies worldwide, producing IoT sensor platforms based on low-power technology, giving smart city solutions emphasizing on the efficient use of public service facilities and smart buildings. Integrated with smart meters and smart sensors for real time monitoring of power distribution, asset location, water consumption/quality, gas emissions/air quality, etc. Blockchain hardware & software solutions allow the companies to securely connect smart devices. Small footprint, ultra-low power/next-generation batteries and wearable IoT optimized products are some extra features to be integrated, many times challenging the laws of physics and drive companies to unusual technological approaches.

The rest of this Section provides a comparison of the partners' actual performance with the technological innovation potential and innovative features that will be developed during the project by all partners of the AMANDA project.

Strengths(+)	Weaknesses(-)
- Experience in low-power and energy harvesting is available	- The coverage of European countries with LPWAN is not (yet) consistent
- Combination of innovative sensors (sensor fusion), self-power features form factor not considered or achieved previously at such integration and functionality levels gives a clear position advantage for the consortium.	- Very limited space on the smartcard for future extensions
- Previous positive interactions between most of the members from the consortium	- Lack of standardization across EU countries regarding low-power wireless connectivity makes it more difficult to explain to end-users and deploy in the field (no single wireless protocol solution)
- World-class efficiency and performance of the 1st generations of components (sensors, Energy harvesting, power management and storage) brought into the project	- Complexity of the ASSC integration will require multiple iterations that will be challenging to solve within the project timeline
- Good tools for analysis of energy requirements	- Sensor/data fusion needs to be clarified with further end-user input during the first phase of project.
- Good contacts with the low-power semiconductor and sensor industry	- Lack of the awareness among stakeholders and difficulties to understand similar solutions
- Use of energy harvesting is especially important for IoT devices and for	- Slow diffusion of knowledge among potential stakeholders due functional disaggregation of the actors in the chain
- Personnel highly qualified in this area of activities with great complementarity of the technical skills	
- Stable economic and financial situation of the partners. Resources already in place for a prompt and efficient project start.	
- Deep knowledge of the market strategies for the individual components.	
- Good initial understanding of the potential exploitation routes for the integrated ASSC	
- Expertise in procedures and methods for protecting intellectual propriety	
- The consortium is the owner of specific innovative technologies	
- Positive results from past and ongoing research activities and projects as well as success stories	
Opportunities(+)	Threats(-)
- Society is positive towards the use of alternative and renewable energy sources (no batteries, less waste)	- Some mobile phone manufacturers have been interested in adding environment sensors
- Small is beautiful. A smart card format is attractive (easy to carry)	- System integrators or other competitors looking into similar concepts for miniaturisation
- Long range communications add a degree of independence to the system	- Changes in the regulations landscape (for example privacy laws) could make the deployment of IoT sensing and tracking devices more difficult than anticipated.
- Sensor fusion will open-up new application opportunities for AMANDA	- Obstacles to fast entry into the market such as lack of knowledge and the time needed to overcome technical and technological barriers
- Air quality sensing in smart sensing is growing due to importance of monitoring and controlling pollution levels	
- The modularity aspect of the ASSC will offer platform flexibility and further reach.	
- Business to Business initial market could transition to Business-to-Consumer market upon identification of suitable application(s).	

Figure 48 SWOT analysis

4.1   CO₂ sensor

The AMANDA project aims to develop a highly miniaturized system with plenty of sophisticated components that will be powered by only tiny amounts of energy. That feature puts sophisticated requirements for its subsystems. It results in the situation that the components that can be directly used for the project do not exist on the market. The CO_2 sensor is no exception.

The IMEC CO_2 sensor consists of a transducing part and readout part. The transducer on the silicon die can be miniaturized, starting at an mm^2 size with a thickness in the range of 1-2mm. Even the smallest commercially available NDIR sensors are significantly bigger and would be too tall for incorporation in the final ASSC. Measuring the impedance of the passive IMEC sensor uses very little power compared to NDIR sensors. For example, the infrared light sources, which consume electricity in the range of 100mW, can only lower their power consumption by using a low measurement frequency. The small size and low power consumption make the IMEC sensor an excellent fit for AMANDA.

The technical solution used for the readout is unique because of the very high levels of integration and the relatively low power usage. The main component of the readout system is the ADUCM350 microcontroller, a configurable impedance network analyser and potentiostat with an Integrated Cortex M3 Core. This microcontroller has a unique analog front-end that allows for impedance spectroscopy.

Figure 49 Analog front-end of the ADUCM350 microcontroller that allows for impedance spectroscopy [45]

The raw data measured by the device does not directly indicate the CO_2 concentration. The device provides data in arbitrary units. Mathematical techniques, such as a linear/exponential fitting or a Fourier analysis, the denoising needs to be used for crucial feature extraction. Existing algorithms need to be enhanced on their efficiency level because the AMANDA project aims for a very low power consumption profile. Thus, unique algorithms and calibration procedures will be developed during the project.

4.2   Capacitive sensor

In the AMANDA system, the capacitive sensor acts as a system wake-up switch or obtains a similar functionality. This means that in the lowest power system sleep mode, essentially only the capacitive sensor is active and waiting for stimuli. To achieve the best battery life, it is of highest importance that the power consumption of the capacitive switch to be as small as possible. Additionally, the restricted space available on the miniaturized smart card requires

the smallest possible footprint of each embedded function, including the capacitive sensor and switch.

The Microdul MS8891 is an ideal starting point for a development that fulfils those require-ments. The MS8891 is the latest Microdul capacitive switch, which is not yet fully released for production. Its main features are listed in Table *n* above. In particular, it exhibits the lowest power consumption of any capacitive switch on the market while providing a reasonably dy-namic touch behaviour.

Further improvements are planned for the AMANDA capacitive touch sensor, such as:
- Self-calibration feature to compensate manufacturing tolerances
- Auto-calibration feature to compensate slowly changing environmental conditions such as temperature, moisture or dirt assembling on the sensor
- Optimize EMC robustness while keeping the power consumption as is or reduce it even further
- Availability as chip-scale package with reflow-capable solder bump technology

4.3   Temperature sensor

Temperature measurement on the AMANDA smart card is used for monitoring the environ-mental temperature, which normally only changes slowly. Therefore, the aim for the AMANDA temperature sensor is to achieve the lowest power consumption possible at low measure-ment repetition rates that equal to one measurement per minute or longer. In this segment, the current MS1088 of Microdul is among the best in its class, just behind the AMS AS6200.

In the development process for AMANDA, the Microdul temperature sensor will be improved in terms of overall power consumption, focusing on the following three key areas:
- Reduction of measurement duration
- Reduction of current consumption during the measurement
- Reduction of static current between the measurements

The temperature sensor will provide additional hardware features, potentially benefiting the AMANDA system:

A bidirectional hardware handshake line, used to trigger a temperature measurement (con-troller -> temperature sensor) and to flag the completion of the measurement (sensor -> con-troller). This reduces power consumption spent for I2C communication (trigger measurement) and allows the controller to sleep without waiting or polling for the completion of the meas-urement but wake up by an interrupt right after the measurement is completed.

A supply voltage monitoring function (battery-end-of-life or EOL) with configurable voltage threshold levels. This feature provides a very low power battery voltage supervision, if the temperature sensor is supplied directly from the battery voltage.

4.4   Data fusion

The ASSC card will integrate several sensors. Some of the sensors require a high sampling rate. It means that the system can generate an increased amount of data. However, data transfer is expensive in terms of energy consumption. Hence, data need to be (at least partly) pro-cessed on the hardware prior to their submission. Only the information that is important to the user should be transferred from the system. That is why data fusion algorithms need to be applied. Data fusion is the process of integrating multiple data sources to produce more consistent, accurate, and useful information than that provided by any individual data source. Used data science techniques highly depend on the specific of the application. In the project, computation methods like the random forest algorithm or the genetic optimization algorithm might be utilized. However, most likely the work will focus on distributed and recursive Bayes-ian optimization to minimize communication overhead and computational costs.

4.5   Energy harvesting

Lightricity is developing a new Photovoltaic (PV) technology especially designed to harvest energy from indoor low lighting environments (>30% efficiency). The innovative and ultra-high efficient technology of Lightricity will make it possible for the consortium to introduce a completely energy-autonomous device that can harvest indoor and outdoor energy to operate the Autonomous Smart Sensing Card (ASSC) in challenging environments. Existing commercially available Silicon-based would not be able to meet the size requirement, due to their poor efficiency indoors. Other emerging technologies such as Die-sensitized or Organic Photovoltaics may exhibit slightly higher performance than Silicon indoors but suffer from stability issues that unlikely to be solved in the short-to-medium term. Lightricity world-class performance of their larger scale energy harvesting prototypes will be a key enabling technology, providing the power requirements of the ASSC.

The small form factor, thickness, high aesthetics (uniformly black) and robustness of the energy harvester will enable new wearable applications and fits perfectly into the sensing card concept. The compatibility with much higher temperature (250°C) will facilitate greatly the manufacturing of the ASSC since the PV component will be assembled with other electronic components during a standard reflow process (SMT compatible).

5   Recommendations

This Section proposes a list of recommendations to give further directions to the Partners developing key components for the ASSC of the AMANDA project.

As a general remark, a non-volatile RAM memory should be added to the ASSC to improve the total energy efficiency of the system. A flash memory requires more power to write data and has limited write cycles, therefore for an application that requires a frequent update of data, a technology like FRAM or ReRAM should be considered instead.

5.1   Storage element

The most important factor to consider for the development of the ASSC for the AMANDA project is the peak required current, ensuring that it can be supported by the energy storage element, designed by ILIKA. Considering the current state of the storage element, its capacity should be increased since it is linearly affecting the peak discharge current.

Considering the peak loads of the ASSC components, the storage element should be scaled up significantly, in order to hold enough energy for the card to be operational during time periods where there is little to no light available, including night hours. The capacity of the element should also be increased as it directly affects the peak and average current that it can provide. At the end of the project, a much higher capacity should be considered that can support the peak currents that any considerable load drawn from the ASSC will require.

5.2 CO_2 sensor

An important load to consider is that of the CO_2 sensor, developed by IMEC. It is the most technologically advanced and the only low power and small footprint sensor available in its field for the ASSC of the AMANDA project, however the current it draws is still considered a challenge; it is in the scale of a few tenths of milli-amperes in conjunction with the measurement time which is in the range of hundreds of milliseconds. Therefore, it is recommended for IMEC to work towards decreasing the active current and also the measurement time of the sensor.

5.3   Imaging sensor

The imaging sensor developed from EPEAS can be used in many use case scenarios and has technical characteristics that make it viable in ultra-low power applications. The sensor currently has a low fps count due to the long frame capturing time which is in the scale of hundreds of milliseconds. The frame capturing time should be reduced in the scale of tens of milliseconds. This will lower the power requirements per frame of the sensor and offer the ability for a higher frame rate to be achieved. The sensor should also be developed to require less power per frame capture if possible.

5.4   Temperature sensor

The temperature sensor developed by MICRODUL should be further developed in order to reduce its measurement time. The sensor has already low energy requirements and a fast start-up time and can been externally powered off effectively zeroing the quiescent current. Emphasis though should be given in lowering the measurement current of the sensor to bring additional energy conservation. When the ASSC is used in use case scenarios that require frequent temperature measurements, the sensor is recommended to have its own autonomous logic and to be able to be programmed with thresholds. It should additionally have the capability to wake up the MCU when these thresholds are crossed.

5.5   Touch sensor

The touch sensor developed by MICRODUL is a great starting point in order to add touch input functionality to the card. Since this is a human interaction sensor it should be always powered to expect interaction from the user. This means that efforts should be given to minimize the current requirements of the sensor if possible.

5.6   Radio transceiver

The biggest current requirement that should be considered as maximum current draw of the system is the transmission current of the radio transceiver. Most LPWAN transceivers proposed by ZHAW require a few tens of milli-amperes for a few tens of seconds to successfully transmit a message in the highest possible transmission power that will offer the best wireless coverage.

5.7   Radio frequency technology

When it comes to the radio frequency technology, the component that fits best each version of the ASSC should be selected, always considering the maximum current that the system can support. For the indoor version of the card, a wireless personal area network like BLE or the 802.15.4 protocol should be used. As discussed in Section 2.7 above, the RSL10 wireless module is a strong contender for the indoor and wearable versions of the ASSC, as is the best in terms of current draw in Personal Area Network type versions and already has a BLE stack available. For the outdoor version of the card, a wide area wireless network technology like LoRa or Sigfox should be considered. Since the LoRa SX1261 chipset has already been tested by ZHAW with good results it is recommended for the outdoor design. The wearable version can be implemented with either radio technology depending on the application. Both recommended technologies have acceptable positioning capability considering their communication range.

5.8   Power harvesting and power management

The power harvester developed by LIGHTRICITY should be made thinner and compatible with an SMD soldering technology in order to become compatible with the mass manufacturing process required for the AMANDA ASSC.

The power management system should be further improved to support a lower minimum harvesting power from the harvester in order to be able to harvest even the tiniest amount of energy available in indoor low light conditions. The efficiency of the harvesting circuit should be increased for low amounts of energy. The efficiency of the LDOs should be maximized for the loads to be supported. Finally, the quiescent current of the power management unit should be minimized since it is one of the loads that must always be on.

5.9   Processing

For the processing unit of the system, an ultra-low power MCU should be selected that requires only a few micro-amperes per MHz of running frequency that additionally can also sleep in a very deep and low power manner requiring a sleeping current in the nano-ampere scale It should also maintain the processing power required to process the data available from the sensors in an efficient manner. Since EPEAS is developing their own MCU for the needs of the project, these considerations should be taken into account during their development process.

6   Conclusions and future work

This Deliverable, D1.1 - SoA and Gap analysis/ recommendations on ESS features report is part of **Task T1.1 – SoA Analysis, feasibility study and benchmarking of best practices**. The Deliverable provides a comprehensive study on the SoA regarding key, cutting edge technologies and components of the ASSC. These components include core sensors such as imaging, capacitive, temperature and CO_2 sensors, MCUs, energy harvesting technologies, batteries and PMICs as well as wireless communication, packaging and PCB design technologies.

The technology of the key AMANDA sensors is compared to different related fields of research and the way the project contributes beyond the SoA is demonstrated. General guidelines on the project are also provided together with a recommend multi-step system flow to adopt an optimal practice approach. A preliminary GAP analysis took place to specify in detail the technological innovation potential of the AMANDA ASSC components. A comparison of the actual performance of Partners' sensors with the innovative features that will be developed during the project by all partners of the AMANDA project was additionally conducted and their feasibility was studied, mainly in terms of required current. Finally, comprehensive recommendations were given for further directions for the Project.

The work conducted in this Deliverable will help in the definition of the system's requirements under **Task T1.1 – System Requirements and Needs,** leading in **Deliverables D1.2 – Initial system requirements specified** and **D1.7 – Architecture design of the AMANDA system delivered (for both breadboard and integrated/miniaturized system)** as well as to **Milestone MS1 – AMANDA systems specifications and Architecture**.

7 Bibliography

[1]   J. Choi, S. Park, J. Cho and E. Yoon, "A 3.4-µw object-adaptive cmos image sensor with embedded feature extraction algorithm for motion-triggered object-of-interest imaging," 2013..

[2]   S. Hanson, Z. Foo, D. Blaauw and D. Sylvester, "A 0.5v sub-microwatt cmos image sensor with pulse-width modulation read-out," 2010.

[3]   J. Choi, J. Shin, D. Kang and D. Park, "A 45.5µW 15fps always-on CMOS image sensor for mobile and wearable devices," 2015.

[4]   D. Bol, G. de Streel, F. Botman, A. K. Lusala and N. Couniot, "A 65-nm 0.5-V 17-pJ/frame pixels DPS CMOS image sensor for ultralow-power SoCs achieving 40-dB dynamic range," 2014.

[5]   P.-F. Rüedi, R. Quaglia, P. Heim, H.-R. Graf, C. Monneron and B. Schaffer, "An Ultra-low-power High Dynamic Range Image Sensor," *CSEM Scientific and Technical Report 2018,* p. 101, 2018.

[6]   N. Couniot, G. d. Streel, F. Botman, A. K. Lusala, D. Flandre and D. Bol, "A 65 nm 0.5 V DPS CMOS Image Sensor With 17 pJ/Frame.Pixel and 42 dB Dynamic Range for Ultra-Low-Power SoCs," *IEEE Journal of Solid-State Circuits,* vol. 50, no. 10, pp. 2419 - 2430, 2015.

[7]   D. G. Chen, F. Tang, M.-K. Law and A. Bermak, "A 12 pJ/Pixel Analog-to-Information Converter Based 816 × 640 Pixel CMOS Image Sensor," *IEEE Journal of Solid-State Circuits,* vol. 49, no. 5, pp. 1210-1222, 2014.

[8]   T. Haine, F. Stas, G. de Streel, C. Gimeno, D. Flandre and D. Bol, "CAMEL: An Ultra-Low-Power VGA CMOS Imager based on a Time-Based DPS Array," 2016.

[9]   Shadwani, M., et.al., "Capacitive Sensing & Its Applications," *International Journal of Engineering Research and General Science,* Vols. Volume 4, Issue 3, pp. 185-193, May-June 2016.

[10]   T. Grosse-Puppendahl, C. Holz, G. Cohn, R. Wimmer, O. Bechtold, S. Hodges and J. R. Smith, "Finding common ground: A survey of capacitive sensing in human-computer interaction," in *CHI Conference on Human Factors in Computing Systems*, 2017.

[11]   A. Braun, T. Dutz and F. Kamieth, "Capacitive sensor-based hand gesture recognition in ambient intelligence scenarios," in *In Proceedings of the 6th International Conference on PErvasive Technologies Related to Assistive Environments*, 2013.

[12]   S. Oh, et.al., "A Dual-Slope Capacitance-to-Digital Converter Integrated in an Implantable Pressure-Sensing System," *IEEE Journal of Solid State Circuits (JSSC),* July 2015.

[13]   Z. Tan, et.al., "A 1.2-V 8.3-nJ CMOS humidity sensor for RFID applications," *IEEE Journal on Solid-State Circuits (JSSC),* pp. 2469-2477, Oct. 2013.

[14]   S. Xia, et.al., "A capacitance-to-digital converter for displacement sensing with 17b resolution and 20 µs conversion time," in *IEEE Int. Solid-State Circuits Conf. (ISSCC)*, 2012.

[15]   S. Jawed, et.al., "A 828µW 1.8V 80dB dynamic-range readout interface for a MEMS capacitive microphone," in *Proc. Eur. Solid-State Circuits Conf. (ESSCIRC)*, 2008.

[16]   N. Narasimman, et.al., "A 1.2 V, 0.84 pJ/conv.-Step ultra-low power capacitance to digital converter for microphone based auscultation," in *IEEE Custom Integrated Circuits Conference (CICC)*, 2017.

[17]   C. Stetco, et.al., "Piezocapacitive Sensing for Structural Health Monitoring in Adhesive Joints," in *IEEE International Instrumentation and Measurement Technology Conference (I2MTC)*, 2019.

[18]   S. Hussaini, et.al., "A 15nW Per Button Noise-Immune Readout IC for Capacitive Touch Sensor," in *IEEE 44th European Solid State Circuits Conference (ESSCIRC)*, 2018.

[19]   H. Ha, et.al., "A 160nW 63.9fJ/conversion-step Capacitance-to-Digital Converter for Ultra-Low-Power Wireless Sensor Nodes," in *IEEE ISSCC*, 2014.

[20]   A. Omran, et.al., "A 35fJ/Step Differential Successive Approximation Capacitive Sensor Readout Circuit with Quasi-Dynamic Operation," in *IEEE Symposium on VLSI Circuits*, 2016.

[21]   H. Xin, et.al., "A 0.1-nW–1-µW Energy-Efficient All-Dynamic Versatile Capacitance-to-Digital Converter," *IEEE Journal of Solid-State Circuits (JSSC),* pp. 1841-1851, Jul. 2019.

[22]   B. Murmann, "ADC Performance Survey 1997-2019 (ISSCC & VLSI Symposium)," Aug. 2019. [Online]. Available: http://web.stanford.edu/~murmann/adcsurvey.html. [Accessed 30 10 2019].

[23]   B. Murmann, "Energy Limits in A/D Converters," May 2012. [Online]. Available: https://indico.cern.ch/event/191624/attachments/273635/382982/murmann20120 525cern.pdf. [Accessed 30 10 2019].

[24]   D. Zhou, et.al., "Systematic Design Optimization of Capacitive Touch Sensor Electrode Patterns," *IEEE Sensors Journal,* Oct. 2019.

[25]   M. Hiraki, et.al., "A Capacitance-to-Digital Converter Integrated in a 32bit Microcontroller for 3D Gesture Sensing," in *IEEE Asian Solid-State Circuits Conference (A-SSCC)*, 2018.

[26]   G. Singh, et.al., "Event-Driven Low-Power Gesture Recognition Using Differential Capacitance," *IEEE Sensors Journal,* Jun. 2016.

[27]   A. Bakker and J. Huijsing, High Accuracy CMOS Smart Temperature Sensors, Springer, 2000.

[28]   A. Aita, et.al., "A CMOS smart temperature sensor with a batch-calibrated inaccuracy of ±0.25°C (3σ) from −70°C to 130°C," in *IEEE International Solid-State Circuits Conference (ISSCC)*, 2009.

[29]   K. Souri, et.al., "A CMOS Temperature Sensor With a Voltage-Calibrated Inaccuracy of ±0.15°C (3σ) from −55 to 125°C," *IEEE Journal of Solid-State Circuits,* pp. 292-301, Jan. 2013.

[30]   M. Pertijs, et. al., "A CMOS Smart Temperature Sensor with a 3σ Inaccuracy of ±0.1°C From -55°C to 125°C," *IEEE Journal of Solid-State Circuits,* pp. 2805-2815, December 2005.

[31]   C.-Y. Ku, et.al., "A Voltage-Scalable Low-Power All-Digital Temperature Sensor for On-Chip Thermal Monitoring," *IEEE Transactions on Circuits and Systems II: Express Briefs,* Oct. 2019.

[32]   D. Truesdell, et. al., "A 640 pW 22 pJ/sample Gate Leakage-Based Digital CMOS Temperature Sensor with 0.25°C Resolution," in *IEEE Custom Integrated Circuits Conference (CICC)*, 2019.

[33]   CO2Meter, "COZIR TM Ultra Low Power Carbon Dioxide Sensor," pp. 4-6.

[34]   ExploIR, "ExplorIR-M Datasheet," [Online]. Available: http://co2meters.com/Documentation/Datasheets/DS_GC_0024_0025_0026_Revise d8.pdf.

[35]   SenseAir,   "LP8   Datasheet,"   [Online].   Available:
        http://co2meters.com/Documentation/Datasheets/DS_SE_0038_Revised8.pdf.

[36]   Telaire,   "T6713   Datasheet,"   [Online].   Available:
        http://www.mouser.com/ds/2/18/AAS-920-634D-Telaire-T6713%20Series-092415-
        web-1076778.pdf.

[37]   Sensirion,   "SCD30   Datasheet,"   [Online].   Available:
        https://www.sensirion.com/fileadmin/user_upload/customers/sensirion/Dokument
        e/0_Datasheets/CO2/Sensirion_CO2_Sensors_SCD30_Datasheet.pdf.

[38]   Cozir,   "GC-0010   Datasheet,"   [Online].   Available:
        http://www.co2meters.com/Documentation/Datasheets/DS-GC-0010-COZIR-
        Ambient.pdf.

[39]   F. USA, "TGS 4161 - for the detection of Carbon Dioxide," pp. 1-2, 2005.

[40]   M. Febrina, E. Satria, M. Djamal and W. Srigutomo, "Development of a simple CO2
        sensor based on the thermal conductivity detection by a thermopile," *Measurement,*
        vol. 133, pp. 139-144, 2019.

[41]   I. M. M.Perez de Vargas-Sansalvador, M. M. Erenas, D. Diamond, B. Quiltyc and L.
        Fermin Capitan-Vallveya, "Water based-ionic liquid carbon dioxide sensor for
        applications in the food industry," *Sensors and Actuators B: Chemical,* vol. 253, pp.
        302-309, 2017.

[42]   L. Chen, D. Huang, S. RenYuwu Chi and G. Chen, "Carbon Dioxide Gas Sensor Based on
        Ionic Liquid-Induced Electrochemiluminescence," *Analytical Chemistry,* vol. 83, no. 17,
        pp. 6862-6867, 2011.

[43]   "New environmental sensor technology: photoacoustic spectroscopy (PAS)
        miniaturizes CO2 sensor XENSIV™ PAS210," Infineon, 2019. [Online]. Available:
        https://www.infineon.com/cms/en/about-infineon/press/market-
        news/2019/INFPMM201906-080.html. [Accessed 02 11 2019].

[44]   "Breakthrough in CO2 Sensing: First Sensirion Miniaturized CO2 Sensor," Sensirion, 05
        07 2019. [Online]. Available: https://www.sensirion.com/en/about-
        us/newsroom/news-and-press-releases/detail/news/breakthrough-in-co2-sensing-
        first-sensirion-miniaturized-co2-sensor/. [Accessed 02 11 2019].

[45]   A. Devices, "16-Bit Precision , Low Power Meter On A Chip with Cortex-M3 and
        Connectivity," 2014.

[46]   "https://www.eembc.org/," [Online].

[47]   C. DeFeo, "Green Information Technology," 13 March 2015.

[48]   enocean, "EnOcean Self-powered IoT - ECS 300," EnOcean, [Online]. Available:
        https://www.enocean.com/en/enocean-modules/details/ecs-300/.

[49]   Panasonic,   "Panasonic-AM-1606C-Datasheet,"   [Online].   Available:
        https://www.mouser.com/ds/2/315/panasonic_AM-1606C-1197092.pdf.

[50]   Panasonic,   "Panasonic-1456CA   Datasheet,"   [Online].   Available:
        https://gr.mouser.com/datasheet/2/315/panasonic_AM-1456CA-1196920.pdf.

[51]   "Eight19,"   [Online].   Available: https://eight19.com/wp-
        content/uploads/2016/08/Indoor-Engineering-Sample-Specs-Sheet-
        E19_ES_7_12_002.pdf.

[52]   "GCell," [Online]. Available: https://gcell.com/product/gcell-sample-dssc-module.

[53]   A. S. Weddell, G. V. Merrett and B. M. Al-Hashimi, "Photovoltaic sample-and-hold
        circuit enabling MPPT indoors for low-power systems," 2012.

[54]　"https://panasonic.co.jp/es/pesam/en/products/pdf/Catalog_Amorton_ENG.pdf,"
[Online].

[55]　G. Lucarelli, F. Di Giacomo, V. Zardetto, M. Creatore and T. M. Brown, "Efficient light
harvesting from flexible perovskite solar cells under indoor white light-emitting diode
illumination," 2017.

[56]　S. Mori, T. Gotanda, Y. Nakano, M. Saito, K. Todori and M. Hosoya, "Investigation of
the organic solar cell characteristics for indoor LED light applications," 2015.

[57]　H. Lee, J. Barbé, S. M. P. Meroni, T. Du, C. Lin, A. Pockett, J. Troughton, S. M. Jain, F. D.
Rossi, J. Baker, M. J. Carnie, M. A. McLachlan, T. M. Watson, J. R. Durrant and W. Tsoi,
"Outstanding Indoor Performance of Perovskite Photovoltaic Cells – Effect of Device
Architectures and Interlayers," *Solar RRL,* vol. 3, no. 1, 23 November 2018.

[58]　"Taiwan researchers develop perovskite solar cells to convert indoor light," 18 April
2019. [Online]. Available: https://www.digitimes.com/news/a20190417PD210.html.
[Accessed 01 November 2019].

[59]　Y. Cui, Y. Wang, J. Bergqvist, H. Yao, Y. Xu, B. Gao, C. Yang, S. Zhang, O. Inganäs, F. Gao
and J. Hou, "Wide-gap non-fullerene acceptor enabling high-performance organic
photovoltaic cells for indoor applications," *Nature Energy,* vol. 4, pp. 768-775, 2019.

[60]　Y. Cao, Y. Liu, S. M. Zakeeruddin and A. Hagfeldt, "Direct Contact of Selective Charge
Extraction Layers Enables High-Efficiency Molecular Photovoltaics," *Joule,* vol. 2, no.
6, pp. 1108-1117, 2018.

[61]　A. Bonfiglio and D. De Rossi, "Wearable Monitoring Systems," 2011.

[62]　H. Kulah and K. Najafi, "Energy Scavenging From Low-Frequency Vibrations by Using
Frequency Up-Conversion for Wireless Sensor Applications," 2008.

[63]　"http://www.getfreevolt.com/," [Online].

[64]　Ilika, *Stereax® M250 Rechargeable Solid State Battery: 250 μAh, 3.5 V.*

[65]　Cymbet, *Rechargeable Solid State Bare Die Batteries.*

[66]　F. K, "Solid State Ionics: from Michael Faraday to green energy-the European
dimension," *Science and Technology of Advanced Materials,* vol. 14, no. 4, 2013.

[67]　NobelPrize.org, "The Nobel Prize in Chemistry 2019," [Online]. Available:
https://www.nobelprize.org/prizes/chemistry/2019/summary/.

[68]　K. S. Jones, N. G. Rudawski, I. Oladeji, R. Pitts and R. Fox, "The state of solid-state
batteries," *American Ceramic Society Bulletin,* vol. 91, no. 2.

[69]　M. A. e. a. Kraft, "Influence of lattice polarizability on the ionic conductivity in the
lithium superionic argyrodites Li6PS5X (X = Cl, Br, I)," *J. Am. Chem. Soc.,* vol. 139, pp.
10909-19018, 2017.

[70]　R. &. M. M. Kanno, "Lithium ionic conductor thio-LISICON: the Li2S-GeS2-P2S5
system.," *J. Electrochem. Soc. ,* vol. 148, pp. A742-746, 2001.

[71]　Y. e. a. Deng, "Structural and mechanistic insights into fast lithium-ion conduction in
Li4SiO4–Li3PO4 solid electrolytes.," *J. Am. Chem. Soc,* vol. 137, pp. 9136-9145, 2015.

[72]　U. o. C. Boulder, "Solid-state battery developed at CU-Boulder could double the range
of electric cars," November 2013. [Online]. Available:
https://web.archive.org/web/20131107054525/https://www.colorado.edu/news/re
leases/2013/09/18/solid-state-battery-developed-cu-boulder-could-double-range-
electric-cars.

[73]　U. o. T. a. Austin, "Lithium-Ion Battery Inventor Introduces New Technology for Fast-
Charging, Noncombustible Batteries," 28 February 2017. [Online]. Available:

https://news.utexas.edu/2017/02/28/goodenough-introduces-new-battery-technology.

[74]   J. M. C. C. M. L. C. &. D. N. Li, "Solid electrolyte: the key for high-voltage lithium batteries.," *Adv. Energy Mater.,* vol. 5, p. 1401408, 2015.

[75]   Z. C. I.-H. D. Z. &. O. S. P. Zhu, "Role of Na+ interstitials and dopants in enhancing the Na+ conductivity of the cubic Na3PS4 superionic conductor.," *Chem. Mater. ,* vol. 27, pp. 8318-8325, 2015.

[76]   MIT News, "Enriching solid-state batteries," 2019. [Online]. Available: http://news.mit.edu/2019/enriching-solid-state-batteries-jennifer-rupp-mit-0711.

[77]   K. H. Y. &. T. N. Yoshima, "Thin hybrid electrolyte based on garnet-type lithium-ion conductor Li7La3Zr2O12 for 12 V-class bipolar batteries," *J. Power Sources,* vol. 302, pp. 283-290, 2016.

[78]   A. H. S. M. H. T. M. &. M. T. Hayashi, "Preparation of Li2S–P2S5 amorphous solid electrolytes by mechanical milling.," *J. Am. Ceram. Soc,* vol. 84, pp. 477-479, 2004.

[79]   J. F. M. B. L. &. N. P. H. L. Oudenhoven, "All-solid-state lithium-ion microbatteries: a review of various three-dimensional concepts.," *Adv. Energy Mater.,* vol. 1, pp. 10-33, 2011.

[80]   M. e. a. Finsterbusch, "High Capacity garnet-based all-solid-state lithium batteries: fabrication and 3D-microstructure resolved modeling.," *ACS Appl. Mater. Interfaces ,* vol. 10, p. 22329–22339, 2018.

[81]   H. Z. a. M. H. A. S. Jian Liu, "Toward 3D Solid-State Batteries via Atomic Layer Deposition Approach," *Front. Energy Res.,* 2018.

[82]   "E-peas semiconductors, Highly-efficient, regulated dual-output, ambient energy manager for up to 7-cell solar panels with optional primary battery," 2018.

[83]   "Texas Instruments, Nano Power Boost Charger and Buck Converter for Energy Harvester Powered Applications," 2013.

[84]   "Texas Instruments, Ultra Low-Power Boost Charger with Battery Management and Autonomous Power Multiplexer for Primary Battery in Energy Harvester Applications," 2013.

[85]   "Analog Devices, Ultralow Power Energy Harvester PMUs with MPPT and Charge Management," 2016.

[86]   "Analog Devices, Ultralow Power Boost Regulator with MPPT and Charge Management," 2014.

[87]   "ST Microelectronics, Ultralow power energy harvester and battery charger," 2013.

[88]   L. Technologies, "400mA Step-Up DC/DC Converter with Maximum Power Point Control and 250mV Start-Up," 2015.

[89]   Cypress, "Ultra Low Voltage Boost PMIC for Solar/Thermal Energy Harvesting," 2015.

[90]   L. Technologies, "Ultralow Voltage Step-Up Converter and Power Manager," 2019.

[91]   "EM microelectronics, Ultra-low voltage dcdc boost converter for thermal electrical generators," 2017.

[92]   G. S. Chandu and R. M. Kumar, "A comparative study on various LPWAN and cellular communication technologies for IoT based smart applications," *2018 International Conference on Emerging Trends and Innovations In Engineering And Technological Research, ICETIETR 2018,* pp. 1-8, 2018.

[93]   I. N. Laili, K. Murizah, I. Mahamod and M. Roslina, "A review of low power wide area technology in licensed and unlicensed spectrum for IoT use cases," *Bulletin of Electrical Engineering and Informatics,* vol. 7, no. 2, pp. 183-190, 2018.

[94]   K. Mekki, E. Bajic, F. Chaxel and F. Meyer, "Overview of Cellular LPWAN Technologies for IoT Deployment: Sigfox, LoRaWAN, and NB-IoT," *2018 IEEE International Conference on Pervasive Computing and Communications Workshops, PerCom Workshops 2018,* pp. 197-202, 2018.

[95]   U. Raza, P. Kulkarni and M. Sooriyabandara, "Low Power Wide Area Networks: An Overview," *IEEE Communications Surveys and Tutorials,* vol. 19, no. 2, pp. 855-873, 2017.

[96]   F. Montori, L. Bedogni, M. Di Felice and L. Bononi, "Machine-to-machine wireless communication technologies for the Internet of Things: Taxonomy, comparison and open issues," *Pervasive and Mobile Computing,* vol. 50, pp. 56-81, 2018.

[97]   Nokia, "LTE-M – Optimizing LTE for the Internet of Things White Paper," *White Paper,* p. 16, 2015.

[98]   T. Rahman and S. K. Chakraborty, "Provisioning technical interoperability within ZigBee and BLE in IoT environment," *2018 2nd International Conference on Electronics, Materials Engineering and Nano-Technology, IEMENTech 2018,* pp. 1-4, 2018.

[99]   M. Meli and R. Kräuchi, "Limitations of Current LP-WAN Systems," 2017.

[100]   M. Brütsch, C. Brülisauer, L. Widmer, R. Kräuchi, D. Truninger and M. Meli, "Comparing the energy requirements of current Bluetooth Smart Devices," 2018.

[101]   M. Gugg, M. Brütsch, C. Brülisauer and M. Meli, "Comparing the energy requirements of current Bluetooth Smart solutions," 2016.

[102]   "Springborn Laboratories for US department of Energy, "Investigation of test methods, material properties, and processes for solar cell encapsulants", p 3-6, 1979".

[103]   D. Karnaushenko, D. Makarov, M. Stöber, D. D. Karnaushenko , S. Baunack and O. G. Schmidt , "High-performance magnetic sensorics for printable and flexible electronics," *Advanced Materials,* vol. 27, no. 5, pp. 880-885, 2015.

[104]   P. Janghoon, L. Jongsu, P. Sungsik, S. Kee Hyun and L. Dongjin, "Development of hybrid process for double-side flexible printed circuit boards using roll-to-roll gravure printing, via-hole printing, and electroless plating," *International Journal of Advanced Manufacturing Technology,* vol. 82, no. 9-12, pp. 1921-1931, 2016.

[105]   A. Sridhar, M. Cauwe, H. Fledderus, R. Kusters and J. Van Den Brand, "Novel interconnect methodologies for ultra-thin chips on foils," *Proceedings - Electronic Components and Technology Conference,* pp. 238-244, 2012.

[106]   [Online]. Available: https://be.eurocircuits.com/shop/orders/configurator.aspx.

[107]   B. O'Flynn, S. Bellis, K. Delaney, J. Barton, S. C. O'Mathuna, A. M. Barroso, J. Benson, U. Roedig and C. Sreenan, "The development of a novel minaturized modular platform for wireless sensor networks," *2005 4th International Symposium on Information Processing in Sensor Networks, IPSN 2005,* vol. 2005, pp. 370-375, 2005.

[108]   D. Moser and J. Krause, "3D-MID - Multifunctional Packages for Sensors in Automotive Applications," *Advanced Microsystems for Automotive Applications 2006,* pp. 369-375, 2006.

[109]   B. Vandevelde, C. Okoro, M. Gonzalez, B. Swinnen and E. Beyne, "Thermo-mechanics of 3D-wafer level and 3D stacked IC packaging technologies," *EuroSimE 2008 - International Conference on Thermal, Mechanical and Multi-Physics Simulation and Experiments in Microelectronics and Micro-Systems,* pp. 1-7, 2008.

[110]   P. Ekkels, "Ultra-thin Packaging Technology (UTCP) for embedding in Flexible substrates," 2016.

[111] D. Nilsson, L. Theuer, V. Beni, P. Dyreklev, P. Norberg, P. Arven, A. P. Turner, J. Wikner and G. Gustafsson, "Combining Electrochemical Bio-sensing, Hybrid Printed Electronics and Wireless Communication for Enabling Real-time and Remote Monitoring of Lactate," p. 5.

[112] P. Chulsung and C. H. Pai, "Eco: Ultra-wearable and expandable wireless sensor platform," *Proceedings - BSN 2006: International Workshop on Wearable and Implantable Body Sensor Networks,* vol. 2006, pp. 162-165, 2006.

[113] B. Matthias, B. Matthias, R. Till and B. Michael, "Poster : bPart - A Small and Versatile Bluetooth Low Energy Sensor Platform for Mobile Sensing," *MobiSys,* vol. 12, 2015.

[114] L. Torsten, C. Kallmayer and R. Aschenbrenner, "Fully integrated EKG shirt based on embroidered electrical interconnections with conductive yarn and miniaturized flexible electronics," *Proceedings - BSN 2006: International Workshop on Wearable and Implantable Body Sensor Networks,* no. March 2014, pp. 23-26, 2006.

[115] J. Aschoff, "Sources of thoughts from temperature regulation to rhythm Research," *Chronobiology International,* vol. 7, no. 3, pp. 179-186, 1990.

[116] G. Wei, E. Sam, N. H. Y. Yin, C. Samyuktha, C. Kevin, P. Austin, F. H. M., O. Hiroki, S. Hiroshi, K. Daisuke, L. D. Hsien, B. G. A., D. R. W. and J. Ali, "Fully integrated wearable sensor arrays for multiplexed in situ perspiration analysis," *Nature,* vol. 529, no. 7587, pp. 509-514, 2016.

[117] [Online].   Available: https://www.bosch-sensortec.com/bst/products/all_products/bme680.

[118] G. W. Valldorf J., "Advanced Microsystes for Automotive Applications 2006," p. 302.

[119] Cypress, [Online]. Available: https://www.cypress.com/products/s6ae10xa-solar-optimized-energy-harvesting-pmic.

[120] Cypress, "CY39C8xx General Purpose Energy Harvesting PMIC," [Online]. Available: https://www.cypress.com/products/cy39c8xx-general-purpose-energy-harvesting-pmic.

[121] Cymbet Corporation, "EnerChip™ EP Universal Energy Harvester Eval Kit," [Online]. Available: https://media.digikey.com/pdf/Data%20Sheets/Cymbet/CBC-EVAL-09.pdf.

[122] Texas Instruments, "Ultra Low Power Harvester Power Management IC with Boost Charger, and Nanopower Buck Converter," [Online]. Available: http://www.ti.com/product/BQ25570.

[123] N. Garg and R. Garg, "Energy harvesting in IoT devices: A survey," Palladam, India, Dec. 2017 .

[124] "ST Microelectronics," [Online]. Available: https://www.st.com/en/power-management/spv1050.html.

[125] "a-Si Wikipedia page," [Online]. Available: https://en.wikipedia.org/wiki/Amorphous_silicon.

[126] "OPV Wikipedia page," [Online]. Available: https://en.wikipedia.org/wiki/Organic_solar_cell.

[127] "DSSC and Perovskites Wikipedia page," [Online]. Available: https://en.wikipedia.org/wiki/Dye-sensitized_solar_cell.